A LATERAL STEERING DYNAMICS MODEL FOR THE DALLAS/FORT WORTH AIRTRANS

Craig C. Smith
Steven Tsao

DRAFT REPORT

DECEMBER 1976

COUNCIL FOR ADVANCED TRANSPORTATION STUDIES

The University of Texas at Austin

A LATERAL STEERING DYNAMICS MODEL FOR THE DALLAS/FORT WORTH AIRTRANS

Craig C. Smith
Steven Tsao

December 1976
RESEARCH REPORT

Prepared for

COUNCIL FOR ADVANCED TRANSPORTATION STUDIES
THE UNIVERSITY OF TEXAS AT AUSTIN
AUSTIN, TEXAS 78712

in cooperation with

U. S. DEPARTMENT OF TRANSPORTATION
OFFICE OF UNIVERSITY RESEARCH
WASHINGTON, D. C. 20590

NOTICE

This document is disseminated under the sponsorship of the Department of Transportation, Office of University Research, in the interest of information exchange. The United States Government and The University of Texas at Austin assume no liability for its contents or use thereof.

Technical Report Documentation Page

1. Report No.	2. Government Accession No.	3. Recipient's Catalog No.
DOT-UT-50126		

4. Title and Subtitle	5. Report Date
A Lateral Steering Dynamics Model for the Dallas/Fort Worth AIRTRANS	December, 1976
	6. Performing Organization Code
7. Author(s) C. C. Smith and S. Tsao	8. Performing Organization Report No. RR-41
9. Performing Organization Name and Address Council for Advanced Transportation Studies The University of Texas at Austin Austin, Texas 78712	10. Work Unit No. (TRAIS) 11. Contract or Grant No. DOT-OS-50126 13. Type of Report and Period Covered Research Report
12. Sponsoring Agency Name and Address U.S. Department of Transportation Office of University Research Washington, D.C. 20590	14. Sponsoring Agency Code

15. Supplementary Notes

16. Abstract

A lateral dynamic steering model of the automatically steered AIRTRANS vehicle at the Dallas/Fort Worth Airport is developed. The general nonlinear model is linearized and presented in a form suitable for ride quality investigation. A set of independent, non-dimensional vehicle parameters is identified. Basic system natural frequencies and modes are identified, and the sensitivity of system response to basic system design parameters is presented. It was found that vehicle steering gain and speed have a greater effect upon vehicle ride quality than other vehicle parameters.

17. Key Words	18. Distribution Statement
Steering Dynamics; Ride Quality; Personal Rapid Transit; Lateral Vehicle Dynamics; Automatic Steering	

19. Security Classif. (of this report)	20. Security Classif. (of this page)	21. No. of Pages	22. Price
Unclassified	Unclassified		

EXECUTIVE SUMMARY

Abstract

A lateral dynamic steering model of the automatically steered AIRTRANS vehicle at the Dallas/Fort Worth Airport is developed in the study. The general nonlinear model is linearized and presented in a form suitable for ride quality investigation. A set of independent, non-dimensional vehicle parameters is identified. Basic system natural frequencies and modes are identified, and the sensitivity of system response to basic system design parameters is presented. It was found that vehicle steering gain and speed have a greater effect upon vehicle ride quality than other vehicle parameters.

Introduction

The acceptance of any new transportation system is affected by the vibrations, or "ride quality," to which passengers are exposed. Since system ride quality is closely related to system cost, however, is important that the ride quality of any new system, with its inherent cost implications, be defined in the planning of the system, and that alternative methods of achieving a given level of ride quality be evaluated.

The Dallas/Fort Worth AIRTRANS system is a "first kind" of new transportation system and is interesting not only in its own right but as a prototype for possible future systems. In this work, a dynamic model is developed which characterizes the principal lateral steering dynamics effects of the Airtrans vehicle. This model can be used to study vehicle design trade-offs or guideway sidewall roughness effects upon ride quality. Simplified models developed herein are also appropriate for use in relating guideway sidewall roughness to ride qualtiy for possible future automatically steered rubber-tired vehicles.

Method

A lumped element, six-degree-of-freedom dynamic model is developed. Equations are developed which are in general nonlinear. The equations are then linearized and presented in both state variable (time domain) and

frequency domain form. Basic modes of vibration are identified and characterized. Predicted vehicle lateral accelerations using two different assumed inputs are compared with measured vehicle accelerations. A reduced four-degree-of-freedom model is introduced with little loss of model accuracy within the frequencies of primary interest. The equations are non-dimensionalized, and a minimum set of independent non-dimensional vehicle parameters is identified. A sensitivity study indicates the vehicle parameters which have the greatest effect upon vehicle ride quality.

Findings and Results

The vehicle acceleration spectra predicted using the model agrees reasonably well with measured vehicle acceleration spectra at frequencies below about 8 hertz, which include the frequencies of primary interest for ride quality considerations. At higher frequencies, effects not included in the model become significant. The dominant (lowest frequency) vibration modes of the steering system include a lateral body displacement mode at about 1.6 hertz and a vehicle yaw mode at about 2.0 hertz. Additional steering system modes occur at about 4.0 hertz. The predicted vehicle output spectra also contain multiple peaks due to "kinematic resonances" which occur when the wavelength of the vehicle steering inputs is an even fraction of the distance between the vehicle guidewheels.

The vehicle design parameters which most strongly affect the vehicle output spectra and therefore the ride quality were found to be the vehicle steering gain and the velocity or speed.

Significant Conclusions

The model herein developed can be a useful tool in the development of new transportation systems. Vehicle parameters most closely related to ride quality include vehicle steering gain and velocity. Additional studies utilizing models of this type will ultimately allow determination of the sensitivity of vehicle ride comfort and system costs.

ACKNOWLEDGMENTS

This work was supported by the U.S. Department of Transportation University Research Office under Contract DOT-OS-50126, administered through the Council for Advanced Transportation Studies at the University of Texas at Austin. Of particular significance in the development of this work were the cooperation and assistance of LTV Aerospace Systems personnel F. E. Dean, S. J. Starr, and B. J. Brock in obtaining system configuration and parameter information. Also helpful was the cooperation of W. Stewart, AIRTRANS Engineering Administrator at the Dallas/Fort Worth Airport.

TABLE OF CONTENTS

LIST OF FIGURES

LIST OF TABLES

NOMENCLATURE

A = guideway roughness constant, defined in equation (49)

$\underline{A}$ = linear system matrix

$\underline{B}$ = linear system input matrix

$\bar{B}_w$ = steering damping ratio

$B_w[\dot{\theta}]$ = wheel assembly damping torque

b_w = wheel assembly damping coefficient

$\bar{C}$ = cornering coefficient ratio

$\bar{C}_t$ = torque coefficient ratio

$\underline{C}$ = damping matrix

$\underline{\bar{C}}$ = non-dimensional damping matrix

$C[\alpha]$ = lateral roadway-tire force

c = tire cornering coefficient

$\underline{c}^T$ = linear system output matrix

$C_t[\alpha]$ = roadway-tire restoring torque

c_t = roadway-tire restoring torque coefficient

C_{uy} = cross spectral density of u and y

$\underline{D}$ = dynamical matrix

$\underline{d}^T$ = matrix (row vector) relating output and time derivative of the state vector, defined in equation (39)

d_1 = one-half distance between guidebars

$\bar{d}_1$ = guidewheel spacing ratio

d_2 = one-half wheel base

f = circular frequency (hertz)

G = transfer function relating in part from one sidewall and output, defined in equation (46)

$\underline{G}$ = second order system input matrix

$\bar{\underline{G}}$ = non-dimensional second order system input matrix

$\underline{g}^T$ = row vector of transfer functions, defined in equation (40)

G_1, G_2, G_3, G_4 = elements of $\underline{g}^T$

I = vehicle mass moment of inertia (includes wheel assemblies)

$\bar{I}$ = vehicle inertia ratio

$\bar{I}_w$ = wheel assembly inertia ratio

I_w = wheel assembly mass moment of inertia (about axis of rotation relative to vehicle body)

$\underline{K}$ = stiffness matrix

$\bar{\underline{K}}$ = non-dimensional stiffness matrix

$K_1[X]$ = force in guidewheel spring

k_1 = guidewheel spring stiffness

$K_2[X]$ = force through guidebar mechanical stops

$\bar{K}_3$ = steering link stiffness ratio

$K_3[X]$ = force in steering link

k_3 = steering link stiffness

$\bar{K}_4$ = coupling stiffness ratio

$K_4[X]$ = funk spring force

k_4 = funk spring stiffness

ℓ = distance ahead of vehicle yaw axis of passenger position

M = mass of vehicle (including wheel assemblies)

$\bar{M}$ = mass ratio

$\underline{M}$ = mass matrix

$\bar{\underline{M}}$ = non-dimensional mass matrix

m = mass of guidebar

n = lever ratio

$\underline{q}$ = vector of non-dimensional system coordinates

$\bar{r}$ = steering link radius ratio

r_1, r_2 = steering link coupling radii

$\underline{u}$ = vector of system inputs

$\bar{V}$ = velocity ratio

w = frequency (radians/sec)

$\bar{w}$ = non-dimensional frequency

w^* = $\sqrt{k_1/m_f}$ normalization frequency

$\underline{x}$ = vector of system state variables

x^* = $\frac{m_f g}{K_1}$ normalization length

X_f = front guidebar displacement

$\bar{X}_f$ = X_f/x^* = non-dimensional front guidebar displacement

X_r = rear guidebar displacement

$\bar{X}_r$ = X_r/x^* = non-dimensional rear guidebar displacement

X_m = vehicle centroid lateral displacement

$\bar{X}_m$ = X_m/x^* = non-dimensional vehicle centroid lateral displacement

$\underline{z}$ = vector of independent system coordinates

α = tire slip angle

ψ = vehicle yaw angle

$\bar{\psi}$ = non-dimensional vehicle yaw angle

$\underline{\eta}$ = vector of non-dimensional system inputs

ζ = critical damping ratio

Θ = wheel assembly steering angle

Θ_f = front wheel steering angle

$\bar{\Theta}_f$ = non-dimensional front wheel steering angle

Θ_r = rear wheel steering angle

$\bar{\Theta}_r$ = non-dimensional rear wheel steering angle

Ω = spacial frequency (cycles/ft)

Subscripts f = front r = rear

PART I

INTRODUCTION

The construction and acceptance of new transportation systems involves a variety of factors. One such factor, which itself is relatively complex, is the vibration to which the system passengers are subjected. This vibration, commonly referred to as the system ride quality, affects the acceptability of the system from the passengers viewpoint. If the ride is "rougher" than conventional modes of transportation, he is likely to rate the new system as "poor." If, on the other hand, the ride is smooth relative to conventional modes, the passenger is pleased and the new system is more likely to be acceptable.

Perhaps the strongest motivation for studying vehicle ride quality is its interrelationship with system cost. The specification of a maximum level of "roughness" of the vehicle ride very strongly affects the system costs. Both guideway and vehicle costs in many cases may be largely controlled by the level of ride quality deemed acceptable for the system.

One of the first new personal rapid transit systems built in this country is the AIRTRANS System at the Dallas/Fort Worth Regional Airport. This completely automated system consists of rubber-tired vehicles automatically steered in a U-shaped concrete guideway. Small guidewheels contact the guideway sidewalls (or parapet walls) and act as followers, which steer the wheels of the vehicle. Lateral vibrations, which (from measured data) include accelerations about twice as large relative to vertical accelerations as in typical automobiles, are therefore influenced by the roughness of the parapet walls and the dynamics of the steering system.

This study involves the development of a mathematical model of the steering dynamics of the AIRTRANS vehicle. The model considers lateral motions only and is intended for use in studying vehicle ride quality as a function of parapet wall roughness and steering dynamics parameters. The vehicle acceleration spectra predicted by the model are compared with measured vehicle acceleration spectra. Basic steering system natural frequencies and modes are identified, and a minimum set of basic nondimensional vehicle parameters is defined. A sensitivity study is also included to indicate the model output sensitivity to various model parameters.

PART II

BASIC STEERING SYSTEM MODEL

In the development of the lateral model of the AIRTRANS vehicle, the following assumptions are made:

1) Lateral motions and vertical motions are independent.

2) Vehicle lateral motions are small motions perpendicular to a straight path. Use of themodel can be justified, however, to study motions about a nominal path where the variation in time of the nominal path of the vehicle as the vehicle moves along the guideway is slow in comparison to the vehicle response time and the variations due to sidewall roughness.

General nonlinear equations of motions will be developed first and will then be linearized for specific applications where appropriate.

General Equations

Dynamics Equations. The basic system model is shown in Fig 1. The model has six degrees of freedom, including lateral displacements of the front (X_f) and rear (X_r) guidebar assemblies, rotation of the front wheel assembly (Θ_f), rotation of the rear wheel assembly (Θ_r), and lateral displacement (X_m) and yaw (ψ) of the vehicle body. The equations of motion are derived by drawing free-body diagrams of the lumped masses (inertias) associated with each degree of freedom and writing second order differential equations applying Newton's law to each free-body diagram. By so doing, the following six differential equations are found (for details see Appendix A):

$$m_f\ddot{X}_f + n_f K_3[n_f(X_f - X_m - d_2\psi) - r_1\Theta_f] + K_2[X_f - X_m - d_1\psi] - K_1[U_1 - X_f] + K_1[X_f - U_2] = 0 \quad (1)$$

$$m_r\ddot{X}_r + n_r K_3[n_r(X_r - X_m + d_2\psi) - r_1\Theta_r] + K_2[X_r - X_m + d_1\psi] - K_1[U_3 - X_r] + K_1[X_r - U_4] = 0 \quad (2)$$

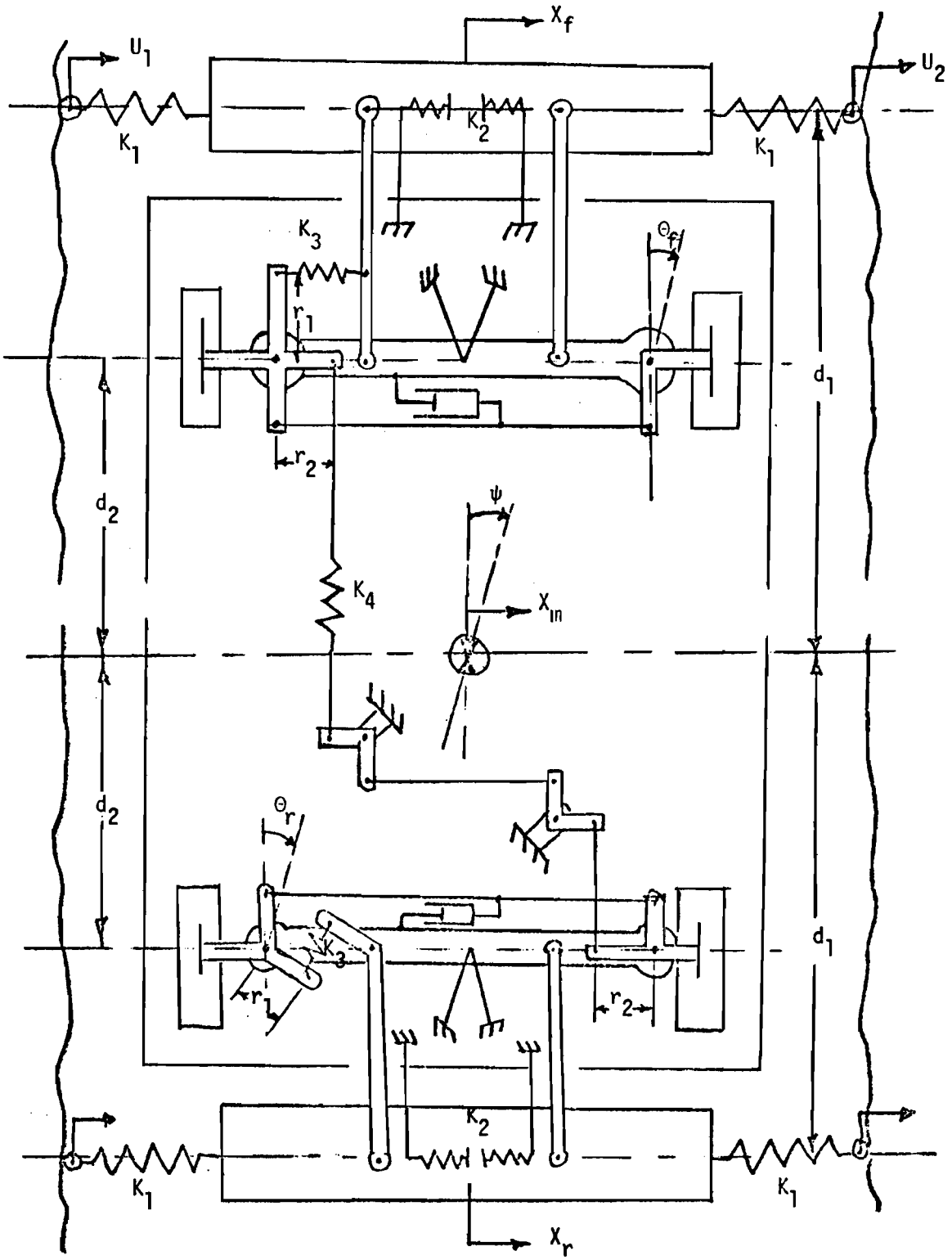

Figure 1. Basic lateral vehicle model.

$$I_w\ddot{\Theta}_f + B_w[\dot{\Theta}_f] + C_t[\Theta_f - \frac{\dot{X}_m + d_2\dot{\psi}}{V}] + r_2K_4[r_2(\Theta_f + \Theta_r)]$$

$$- r_1K_3[n_f(X_f - X_m - d_2\psi) - r_1\Theta_f] = 0 \qquad (3)$$

$$I_w\ddot{\Theta}_r + B_w[\dot{\Theta}_r] + C_t[\Theta_r - \frac{\dot{X}_m - d_2\dot{\psi}}{V}] + r_2K_4[r_2(\Theta_f + \Theta_r)]$$

$$- r_1K_3[n_r(X_r - X_m + d_2\psi) - r_1\Theta_r] = 0 \qquad (4)$$

$$M\ddot{X}_m - C[\Theta_f - \frac{\dot{X}_m + d_2\dot{\psi}}{V}] - C[\Theta_r - \frac{\dot{X}_m - d_2\dot{\psi}}{V}]$$

$$- n_fK_3[n_f(X_f - X_m - d_2\psi) - r_1\Theta_f]$$

$$- n_rK_3[n_r(X_r - X_m + d_2\psi) - r_1\Theta_r]$$

$$- K_2[X_f - X_m - d_1\psi] - K_2[X_r - X_m + d_1\psi] = 0 \qquad (5)$$

$$I\ddot{\psi} - d_2C[\Theta_f - \frac{\dot{X}_m + d_2\dot{\psi}}{V}] + d_2C\ \Theta_r - \frac{\dot{X}_m - d_2\dot{\psi}}{V}]$$

$$- d_1K_2[X_f - X_m - d_1\psi] + d_1K_2[X_r - X_m + d_1\psi]$$

$$- B_w[\dot{\Theta}_f] - [B_w]\dot{\Theta}_r - 2r_2K_4[r_2(\Theta_f + \Theta_r)]$$

$$- (d_1n_f - r_1)\ K_3[n_f(X_f - X_m - d_2\psi) - r_1\Theta_f]$$

$$+ (d_1n_r + r_1)\ K_3[n_r(X_r - X_m - D_2\psi) - r_1\Theta_r] = 0 \qquad (6)$$

In the above equations K_1, K_2, K_3, K_4, C, C_t and B_w are written as operators (or functions). For instance, $C[\alpha]$ denotes the lateral force from the road acting on the tires of a wheel assembly, and $C_t[\alpha]$ is the restoring torque, when the instantaneous slip angle of the tires is α. Similarly, $K_1[X]$, $K_2[X]$, $K_3[X]$, and $K_4[X]$ represent spring forces when each spring deflection is equal to the argument X and $B_w[\omega]$ represents the wheel assembly damping torque as a function of the angular velocity of the wheel assembly. The functional relationships, or constitutive relationships, denoted by the above operators are discussed subsequently.

For computation purposes, it is convenient to write the above equations in state variable form. Defining a set of state variables and state vector as

$$\underline{x} = \begin{bmatrix} X_f \\ X_r \\ \Theta_f \\ \Theta_r \\ X_m \\ \psi \\ \dot{X}_f \\ \dot{X}_r \\ \dot{\Theta}_f \\ \dot{\Theta}_r \\ \dot{X}_m \\ \dot{\psi} \end{bmatrix} = \begin{bmatrix} X_1 \\ X_2 \\ X_3 \\ X_4 \\ X_5 \\ X_6 \\ X_7 \\ X_8 \\ X_9 \\ X_{10} \\ X_{11} \\ X_{12} \end{bmatrix} \tag{7}$$

the above equations can be written in terms of the state variables as follows:

$$\dot{X}_1 = X_7 \quad \dot{X}_2 = X_8 \quad \dot{X}_3 = X_9 \quad \dot{X}_4 = X_{10} \quad \dot{X}_5 = X_{11} \quad \dot{X}_6 = X_{12} \tag{8}$$

$$\dot{X}_7 = -\frac{n_f}{m_f} K_3[n_f(X_1 - X_5 - d_2X_6) - r_1X_3] - \frac{1}{m_f} K_2[X_1 - X_5 - d_1X_6]$$

$$+ \frac{1}{m_f} K_1[U_1 - X_1] - \frac{1}{m_f} K_1[X_1 - U_2] \tag{9}$$

$$\dot{X}_8 = -\frac{n_r}{m_r} K_3[n_r(X_2 - X_5 + d_2X_6) - r_1X_4] - \frac{1}{m_r} K_2[X_2 - X_5 + d_1X_6]$$

$$+ \frac{1}{m_r} K_1[U_3 - X_2] - \frac{1}{m_r} K_1[X_2 - U_4] \tag{10}$$

$$\dot{X}_9 = -\frac{1}{I_w} B_w[X_9] - \frac{1}{I_w} C_t [X_3 - \frac{1}{V}(X_{11} + d_2X_{12})]$$

$$- \frac{r_2}{I_w} K_4[r_2(X_3 + X_4)] + \frac{r_1}{I_w} K_3[n_f(X_1 - X_5 - d_2X_6) - r_1X_3] \quad (11)$$

$$\dot{X}_{10} = -\frac{1}{I_w} B_w[X_{10}] - \frac{1}{I_w} C_t[X_4 - \frac{1}{V}(X_{11} - d_2X_{12})]$$

$$- \frac{r_2}{I_w} K_4[r_2(X_3 + X_4)] + \frac{r_1}{I_w} K_3[n_r(X_2 - X_5 + d_2X_6) - r_1X_4] \quad (12)$$

$$\dot{X}_{11} = \frac{1}{M} C[X_3 - \frac{1}{V}(X_{11} + d_2X_{12})] + \frac{1}{M} C[X_4 - \frac{1}{V}(X_{11} - d_2X_{12})]$$

$$+ \frac{n_f}{M} K_3[n_f(X_1 - X_5 - d_2X_6) - r_1X_3]$$

$$+ \frac{n_r}{M} K_3[n_r(X_2 - X_5 + d_2X_6) - r_1X_4]$$

$$+ \frac{1}{M} K_2[X_1 - X_5 - d_1X_6] + \frac{1}{M} K_2[X_2 - X_5 + d_1X_6] \quad (13)$$

$$\dot{X}_{12} = \frac{d_2}{I} C[X_3 - \frac{1}{V}(X_{11} + d_2X_{12})] - \frac{d_2}{I} C[X_4 - \frac{1}{V}(X_{11} - d_2X_{12})]$$

$$+ \frac{d_1}{I} K_2[X_1 - X_5 - d_1X_6] - \frac{d_1}{I} K_2[X_2 - X_5 + d_1X_6]$$

$$+ \frac{1}{I} B_w[X_9] + \frac{1}{I} B_w[X_{10}] + 2\frac{r_2}{I} K_4[r_2(X_3 + X_4)]$$

$$+ \frac{1}{I}(d_1n_f - r_1) K_3[n_f(X_1 - X_5 - d_2X_6) - r_1X_3]$$

$$- \frac{1}{I}(d_1n_r + r_1) K_3[n_r(X_2 - X_5 + d_2X_6) - r_1X_4] \quad (14)$$

The above state equations can be integrated numerically using a Runge-Kutta or other numerical integration scheme. Using a Runge-Kutta

numerical integration scheme, the acceleration of the vehicle to a step change in the parapet wall surface is given as an example in Part II.

System Output Equations. The system equations (8-14) define the system behavior subject to the input guideway profiles. Any variable of interest (defined as system output) can be written as a function of the system state variables and inputs. For the purpose of studying vehicle ride quality, the most likely variable of interest is the lateral acceleration of the vehicle at a passenger location. For a passenger position located a distance ℓ ahead of the center (yaw axis) of the vehicle, the lateral acceleration (for small yaw angles) is

$$y = \ddot{X}_m + \ell\ddot{\psi} \tag{15}$$

Substituting for $\ddot{X}_m$ and $\ddot{\psi}$ in terms of state variables,

$$\begin{aligned} y = \dot{X}_{11} + \ell\dot{X}_{12} &= \left(\frac{1}{M} + \frac{\ell d_2}{I}\right) C\left[X_3 - \frac{1}{V}(X_{11} + d_2X_{12})\right] \\ &+ \left(\frac{1}{M} - \frac{\ell d_2}{I}\right) C\left[X_4 - \frac{1}{V}(X_{10} - d_2X_{12})\right] \\ &+ \left(\frac{n_f}{M} + \frac{\ell d_1 n_f}{I} - \frac{\ell r_1}{I}\right) K_3[n_f(X_1 - X_5 - d_2X_6) - r_1X_3] \\ &+ \left(\frac{n_r}{M} - \frac{\ell d_1 n_r}{I} - \frac{\ell r_1}{I}\right) K_3[n_r(X_2 - X_5 + d_2X_6) - r_1X_4] \\ &+ \left(\frac{1}{M} + \frac{\ell d_1}{I}\right) K_2[X_1 - X_5 - d_1X_6] + \left(\frac{1}{M} - \frac{\ell d_1}{I}\right) K_2[X_2 - X_5 + d_1X_6] \\ &+ \frac{\ell}{I} B_w[X_9] + \frac{\ell}{I} B_w[X_{10}] + \frac{2\ell r_2}{I} K_4[r_2(X_3 + X_4)] \end{aligned} \tag{16}$$

Elemental Constitutive Relationships

The constitutive relationships or nature of the operators in the above equations may be assumed to be very simple or very complex, depending upon the use and accuracy desired of the model. Typical forms of these functions are described below.

Guidewheel Spring, K_1. The force-deflection relationship for the spring between the guidewheel and guidebar has some nonlinearities by necessity. When the guidewheel is not in contact with the parapet wall, the force applied by the parapet wall is zero and is not a function of guidebar motion. Additionally, it is desirable from a design standpoint to have mechanical stops at each end of the spring stroke to limit the total stroke. This causes the spring to have some preload when the guidewheel is not in contact with the guideway, requiring that the contact force be larger than some nominal value as the guidewheel and guidebar come together before additional spring deflection occurs. At the other end of the stroke, the effective stiffness of the spring increases sharply as the stop is encountered. A typical force-deflection relationship which results from this sort of action is shown in Figure 2. Additionally, other nonlinearities could be designed into the system to attempt to improve system performance, and some were examined during the development of the AIRTRANS vehicle by LTV personnel.[1] However, the relationahip shown in Figure 2 is assumed to be a reasonable representation of the present vehicle now in use.

Guidebar Mechanical Stops, K_2. To avoid excessively large excursions of the guidebar relative to the vehicle body, stops are provided when deflections exceed ± 1.75 inches either side of the center of the vehicle. This effect is modeled as spring K_2 and the resulting constitutive relationship is shown in Figure 3.

Steering Link Flexibility, K_3. The flexibility in the steering link is modeled in Figure 1 as K_3 and is a relatively stiff spring with a stiffness of about 40,000 lbf/in. This spring is generally linear throughout the ranges of interest considered in this study.

Funk Spring Coupling Front and Rear Steering Assemblies. Since the rear guidebar is located behind the rear wheels, it cannot convey information to the rear wheels concerning where the guideway "is going" (relative

---

[1]Personal communication with F. W. Dean, LTV Aerospace Corporation, Dallas, Texas.

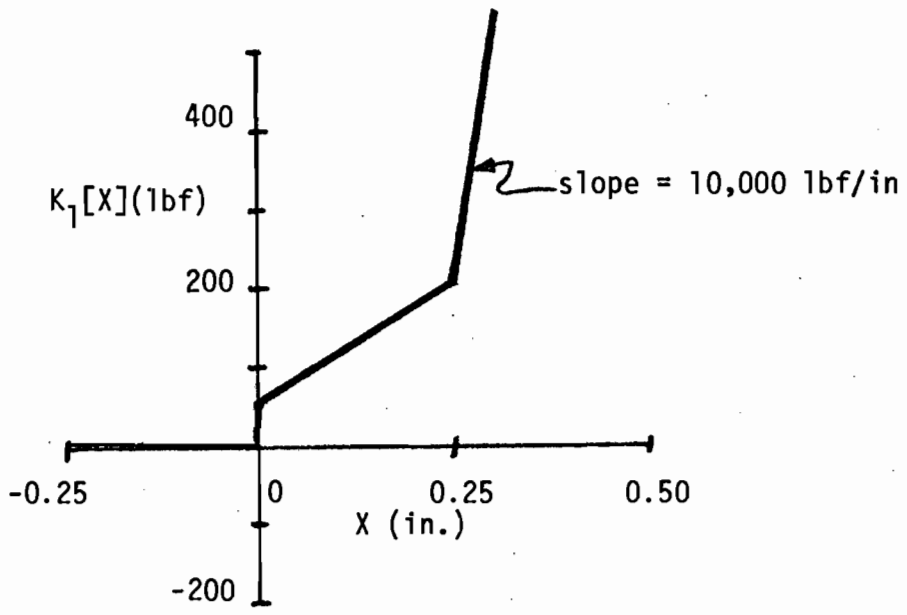

Figure 2 Force-deflection relationship of guidewheel spring K_1

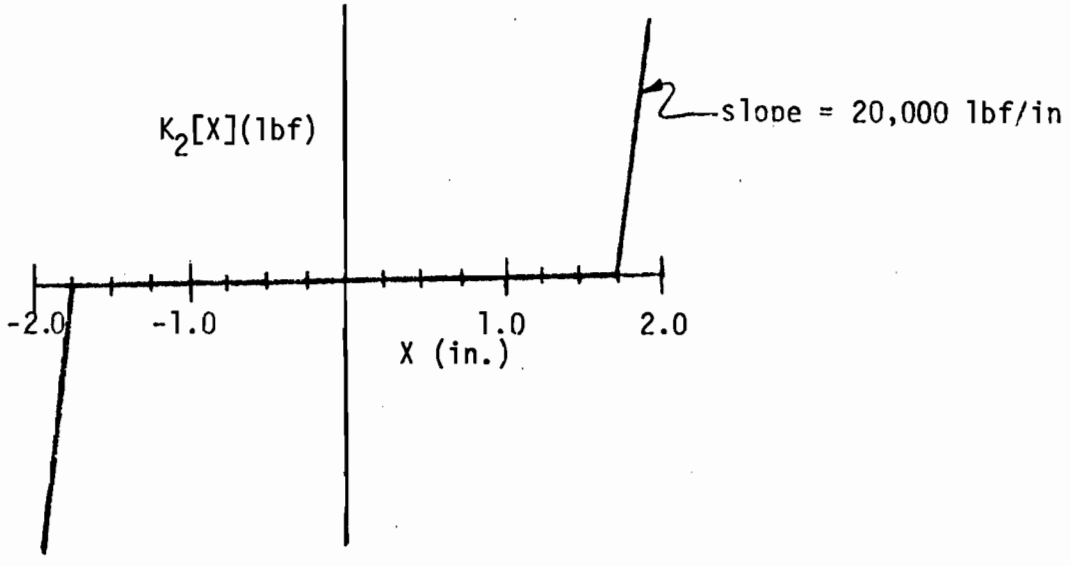

Figure 3. Force-deflection relationship of guidebar mechanical stops K_2.

to the rear wheels) but only where it "has been." It is therefore necessary to couple the front and rear wheel (and/or guidebar) assemblies to cause the rear wheels to follow the path of the front wheels. This coupling is provided by means of the spring K_4 shown in Figure 1. By design, this spring was developed to be piecewise linear, being relatively stiff for small deflections and somewhat softer for larger deflections. The resulting force vs. deflection arrangement is shown in Figure 4. The action of this spring is to provide relatively close coupling between the front and rear steering assemblies when the motions are small. In the event that the rear of the vehicle becomes very largely misaligned with the guideway, however, the front-rear coupling becomes much softer relative to the rear guidebar effect, and the larger corrective action comes through the rear guidebar assembly.

Lateral Force in Road-Tire Interface, $C(\alpha)$. The lateral force developed between a tire and the roadway is a function of the slip angle,* i.e., the angle between the velocity of the tire and the diametral plane of the tire.[2] For small slip angles within some frequencies it is appropriate to consider the force to be simply proportional to the slip angle. For large amplitudes and for high frequencies relative to the rotation speed of the tire, a simple proportionality relationship is no longer valid. For the purposes of this study, the slip angle should remain small, in which case the relationship should remain linear. If the frequencies of interest warrant closer refinement of the model, the range of applicability can be extended by including a second order (which makes C a second order differential operator) model for this interface. This procedure would therefore add two more state variables to the system model and will be investigated should it be deemed necessary as the study progresses. In any case, the function $C[\alpha]$ in the equations above is the combined force on two tires, each assumed to share half the load.

---

*Camber, caster, and vertical and tractive forces on the tire also affect the lateral force but are here considered to be constant.

[2]S. K. Clark, Editor, "Mechanics of Pneumatic Tires," NBS Monograph 122, November 1971.

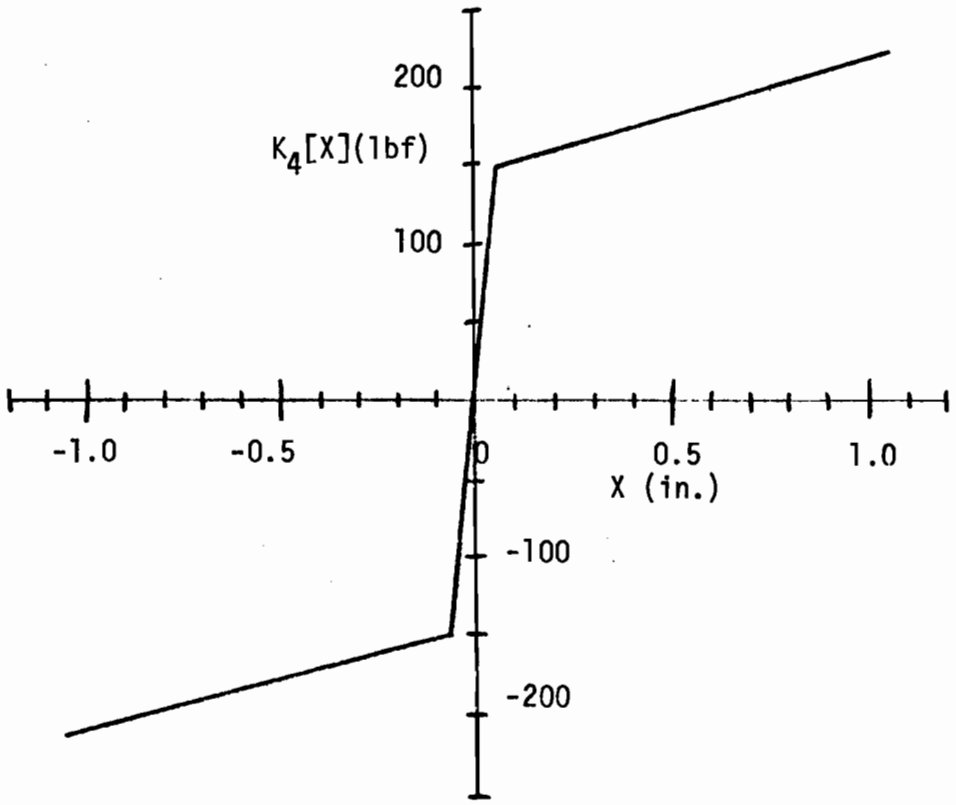

Figure 4. Force-deflection relationship of funk spring K_4 coupling front and rear steering assemblies.

Tire Aligning Torque, $C_t[\alpha]$. The restoring torque applied to a tire by the roadway is also considered to be a function of the tire slip angle, the mechanism being similar to the generation of the lateral force above. Again, $C_t[\alpha]$ is the combined torque applied to both tires in an assembly, each having the same slip angle and sharing half the load.

Steering Assembly Damping, $B_w[\dot{\theta}]$. Damping of the steering assembly is accomplished through a dashpot connected between the steering drag link and the vehicle chassis. This damping is primarily viscous damping and is linear (torque proportional to angular velocity of the wheel assembly) for small angles of the wheel assembly. Additionally, some dry or coulomb friction should be expected at pivot joints, etc., and these effects could also be lumped into the function $B_w[\dot{\theta}]$.

Linear Equations

For many studies, it is appropriate to use a linear approximation to the above equations to facilitate study of basic effects and ease of solution of equations. The linear model can be considered a reasonable approximation for motions small in amplitude and limited in frequency content, the ranges and limitations depending upon the nature of the model.

Making the assumptions that $K_1[X] = k_1X$, $K_2[X] = 0$, $K_3[X] = k_3X$, $K_4[X] = k_4X$, $C[\alpha] = c\alpha$, $C_t[\alpha] = c_t\alpha$, $B_w[\dot{\theta}] = b_w\dot{\theta}$, (17)

equations 1 through 6 can be written in the matrix form

$$\underline{M}\ddot{\underline{z}} + \underline{C}\dot{\underline{z}} + \underline{K}\underline{z} = \underline{G}\underline{u} \tag{18}$$

where $\underline{z} = \begin{Bmatrix} X_f \\ \ell_r \\ \Theta_f \\ \Theta_r \\ X_m \\ \psi \end{Bmatrix}$, $\underline{u} = \begin{Bmatrix} u_1 \\ u_2 \\ u_3 \\ u_4 \end{Bmatrix}$

The $\underline{M}$, $\underline{C}$, $\underline{K}$, and $\underline{G}$ matrices are tabulated in Appendix B.1.

For computational purposes, it is often convenient to write the second order matrix differential equation (18) in the first order form

$$\dot{\underline{x}} = \underline{A}\underline{x} + \underline{B}\underline{u} \tag{19}$$

where the state vector

$$\underline{x} = \begin{Bmatrix} \underline{z} \\ \dot{\underline{z}} \end{Bmatrix} \tag{20}$$

and where the system matrix

$$\underline{A} = \begin{bmatrix} \underline{0} & \underline{I} \\ -\underline{M}^{-1}\underline{K} & -\underline{M}^{-1}\underline{C} \end{bmatrix} \tag{21}$$

and input matrix

$$\underline{B} = \begin{bmatrix} \underline{0} \\ \underline{M}^{-1}\underline{G} \end{bmatrix} \tag{22}$$

are formed using the matrices in (18) as appropriate partitions. Additionally, substituting the linear relationships,(17),into the output equation,(16), yields the linear output equation:

$$\begin{aligned} y = {} & \left\{\frac{n_f^2 k_3}{M} + \frac{(d_1 n_f - r_1) n_f \ell k_3}{I}\right\} X_1 + \left\{\frac{n_r^2 k_3}{M} - \frac{(d_1 n_r + r_1) n_r \ell k_3}{I}\right\} X_2 \\ & + \left\{\frac{c - n_f r_1 k_3}{M} + \frac{\ell d_2 c - \ell d_1 n_f r_1 k_3 + \ell r_1^2 k_3 + 2\ell r_2^2 k_4}{I}\right\} X_3 \\ & + \left\{\frac{c - n_r r_1 k_3}{M} + \frac{-\ell d_2 c + \ell d_1 n_r r_1 k_3 + \ell r_1^2 k_3 + 2\ell r_2^2 k_4}{I}\right\} X_4 \\ & - \left\{\frac{(n_f^2 + n_r^2) k_3}{M} + \frac{d_1 (n_f^2 - n_r^2) \ell k_3 - r_1 (n_f + n_r) \ell k_3}{I}\right\} X_5 \\ & - \left\{\frac{(n_f^2 - n_r^2) d_2 k_3}{M} + \frac{d_1 d_2 \ell (n_f^2 + n_r^2) k_3 + d_2 r_1 \ell (n_r - n_f) k_3}{I}\right\} X_6 \\ & + \frac{\ell b_w}{I} X_9 + \frac{\ell b_w}{I} X_{10} - \frac{2c}{MV} X_{11} - \frac{2cd_2\ell}{IV} X_{12} \end{aligned} \tag{23}$$

which can be written in the matrix form

$$y = \underline{c}^T \underline{x} \tag{24}$$

where $\underline{c}^T$ is tabulated in Appendix B.1.

Comparison of Linear and Nonlinear Model Responses to a Step Input

Solution of the equations representing the system model for the purpose of studying ride quality can be accomplished by a variety of methods. Selection of any particular method depends upon the type of input to be considered, the required accuracy, and the desired form of the output; thus, some trade-off is involved. If the system nonlinearities must be fully represented, the only alternative is to numerically integrate the system equations for any desired input. If, on the other hand, a linear form of the system model can be considered adequate within the range of consideration, a variety of more convenient and efficient solution techniques present themselves.[3] Since the guideway roughness profile inputs and motion acceleration outputs typically of interest in simulation of ride quality are limited in both amplitude and frequency content, a linear model is expected to be adequate for many situations. The range of validity of the linear model can be investigated by comparison of the calculated responses using the linear and nonlinear models with some selected types of inputs. Here the response of the linearized model with parameters listed in Table 1, which were estimated from the constitutive relationships defined previously, is compared with the response of the nonlinear model for an input consisting of a 0.25-in. step in the guideway parapet walls. In other words, both left and right walls were assumed to have a 0.25-in. step at the location of the front guidewheel at $t = 0$. With the vehicle traveling at 25 ft. per second, the rear guidewheels approach the step at about $t = 0.72$ sec. The resulting lateral acceleration at a point 48 inches ahead of the vehicle center for both linear and nonlinear simulations is shown in Figure 5. As can be seen the two agree

---

[3] Mike Pen-Mu Kao, "Vehicle Ride Quality Simulation - FFT vs. Time Domain," Master's Thesis, Department of Mechanical Engineering, The University of Texas at Austin, 1975.

TABLE 1 LINEAR SYSTEM PARAMETERS FOR AIRTRANS VEHICLE

c = 600 lbf/deg = 34,400 lbf/rad

c_t = 2000 in lbf/deg = 114,600 in lbf/rad

d_1 = 108 inches

d_2 = 85 inches

I = 197,700 lbf in sec^2

I_w = 323 lbf in sec^2

k_1 = 400 lbf/in

k_2 = 0

k_3 = 40,000 lbf/in

k_4 = 400 lbf/in

ℓ = 48 inches

M = 14,500 lbm = 37.5 lbf sec^2/in

m_f = 510 lbf = 1.32 lbf sec^2/in

m_r = 510 lbf = 1.32 lbf sec^2/in

n_f = 0.35

n_r = 0.35

r_1 = 8 inches

r_2 = 8 inches

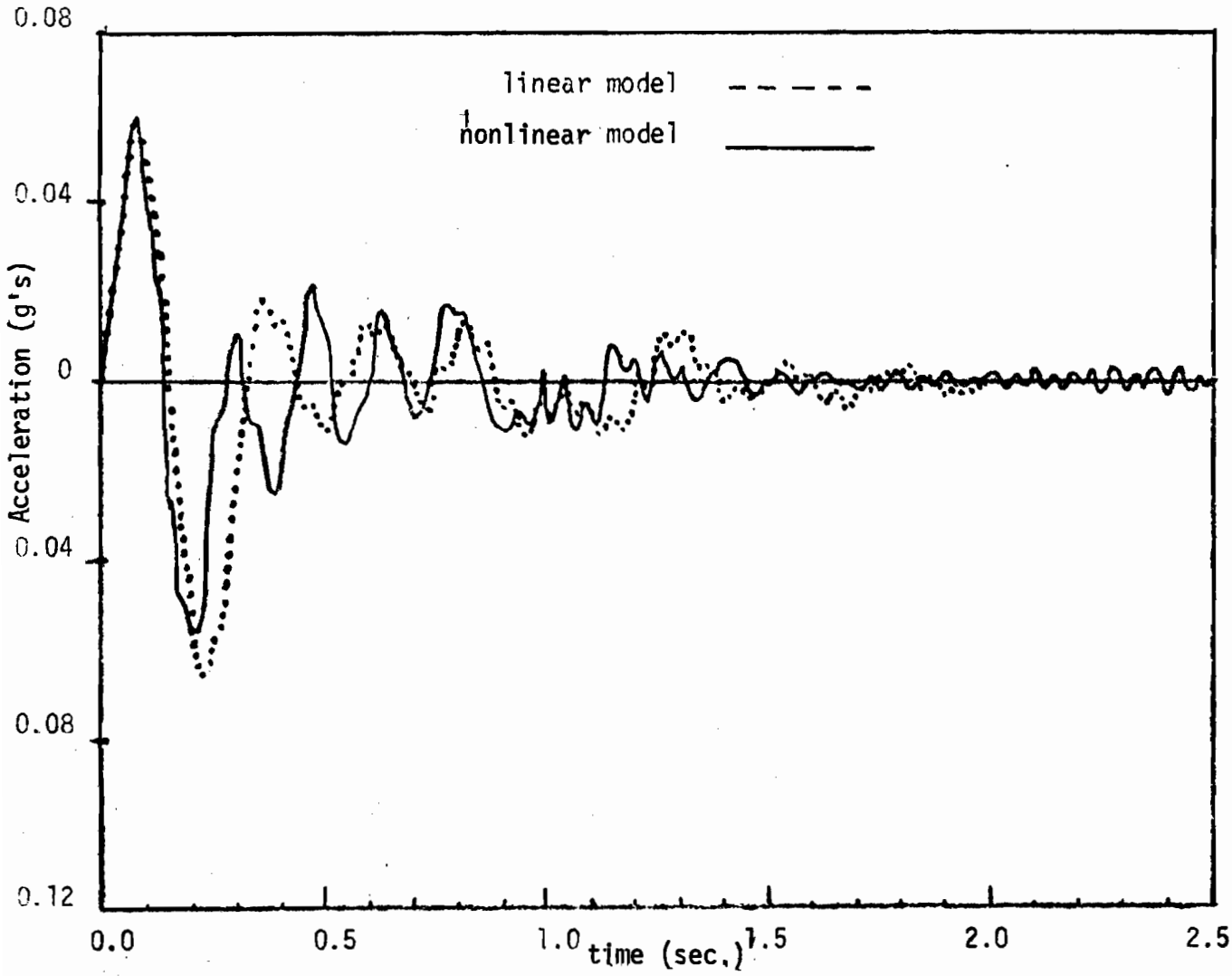

Figure 5. Comparison of passenger position acceleration responses of linear and nonlinear models to a 0.25-inch step change in the guideway.

reasonably well. The basic frequency content of the step response of the linear model appears to be slightly lower than the frequency content of the nonlinear response. Although it is possible that the linearized parameters could be chosen such that the linear and nonlinear responses shown in Figure 5 were in even better agreement, it is noted that the values of the parameters for the "best" agreement is in general a function of the input. The results shown in Figure 5 do serve to give some comparison between the linear and nonlinear models, however, and lend some justification to the use of the linear model in ride quality simulations.

Non-Dimensionalization of System Equations

When dealing with systems with the number of system parameters of the one here considered, it is useful to examine the problem to determine the minimum number of basic independent parameters. This is accomplished by non-dimensionalization of the system equations. At the same time it is useful to normalize the system variables to allow easy comparison between corresponding excursions of the variables.

With the definition of $x^* = \frac{m_f g}{k_1}$ and basic frequency $w^* = \sqrt{k_1/m_f}$, the system normalized non-dimensional variables are defined in Table 2 and are functions of non-dimensional time $\tau = w^* t$. The linear system equations,(18),are then found in the non-dimensional form

$$\bar{M}\ddot{q} + \bar{C}\dot{q} + \bar{K}q = \bar{G}\eta \tag{25}$$

where q is the vector of normalized non-dimensional variables:

$$q = \begin{bmatrix} \bar{X}_f \\ \bar{X}_r \\ \bar{\theta}_f \\ \bar{\theta}_r \\ \bar{X}_m \\ \bar{\psi} \end{bmatrix} \tag{26}$$

where the variables are as defined in Table 2 and where η is the vector of

TABLE 2 NORMALIZED NON-DIMENSIONAL SYSTEM VARIABLES

Variable	Definition
$\bar{X}_f$	X_f/x^*
$\bar{X}_r$	X_r/x^*
$\bar{\theta}_f$	$(\theta_f r_\eta)/x^*$
$\bar{\theta}_r$	$(\theta_r r_\eta)/x^*$
$\bar{X}_m$	X_m/x^*
$\bar{\psi}$	$(\psi d_1)/x^*$

$$x^* = \frac{m_f g}{k}$$

inputs in non-dimensional form

$$\underline{n} = (\frac{1}{X^*})\underline{u} \tag{27}$$

and where the $\underline{\bar{M}}$, $\underline{\bar{C}}$, $\underline{\bar{K}}$, and $\underline{\bar{G}}$ matrices are the non-dimensional mass, stiffness, and input matrices defined in Appendix B.2 and are functions of the system basic non-dimensional parameters listed in Table 3. In the derivation of the basic non-dimensional parameters listed in Table 3, it has been assumed that $m_r = m_f$, $r_2 = r_1 = r$, and $n_f = n_r = n$. These twelve basic non-dimensional parameters represent a minimum set of independent system parameters which describe the system.

Four Degree-of-Freedom Model

Since the stiffness of the steering links, represented by the springs K_3 in Figure 1, is relatively high, the order of the model can be reduced by assuming K_3 to be rigid (infinite stiffness). This can be done with little loss in accuracy at low frequencies (i.e., frequencies below 10-12 hertz, as will be shown later). Assuming K_3 to be rigid, appropriate constraint equations are written as

$$X_f = \frac{r_1}{n_f}\theta_f + X_m + d_2\psi \tag{28}$$

and

$$X_r = \frac{r_1}{n_r}\theta_r + X_m - d_2\psi \tag{29}$$

Substituting these two constraint equations and appropriately modifying the derivation of equations (see details in Appendix C.1), the linear four-degree-of-freedom system equations can be written in the form

$$\underline{M}\ddot{\underline{z}} + \underline{C}\dot{\underline{z}} + \underline{K}\underline{z} = \underline{G}\underline{u} \tag{30}$$

where for this case the vector of system coordinates

$$\underline{z} = \begin{bmatrix} \theta_f \\ \theta_r \\ X_m \\ \psi \end{bmatrix} \tag{31}$$

TABLE 3 BASIC NON-DIMENSIONAL SYSTEM PARAMETERS

Parameter	Symbol	Definition
Steering Link Stiffness Ratio	$\bar{K}_3$	K_3/K_1
Coupling Stiffness Ratio	$\bar{K}_4$	K_4/K_1
Guidewheel Spacing Ratio	$\bar{d}_1$	d_1/d_2
Steering Link Radius Ratio	$\bar{r}$	r/d_2
Steering Lever Ratio	n	ℓ_1/ℓ_2
Wheel Assembly Inertia Ratio	$\bar{I}_w$	$I_w/(r^2 m_f)$
Vehicle Inertia Ratio	$\bar{I}$	$I/(r^2 m_f)$
Steering Damping Ratio	$\bar{B}_w$	$b_w/(r^2 m_f w^*)$
Mass Ratio	$\bar{M}$	M/m_f
Cornering Coefficient Ratio	$\bar{C}$	$(cd_2)/(r^2 m_f w^{*2})$
Torque Coefficient Ratio	$\bar{C}_t$	$c_t/(r^2 m_f w^{*2})$
Velocity Ratio	$\bar{V}$	$V/(d_2 w^*)$

$$w^* = \sqrt{k_1/m_f}$$

$\underline{u}$ is the vector of sidewall profile inputs as defined previously, and where the M, C, and K matrices are the 4 X 4 mass, damping, and stiffness matrices defined in Appendix C.2. In normalized non-dimensional form, these equations can be written

$$\bar{\underline{M}}\ddot{\underline{q}} + \bar{\underline{C}}\dot{\underline{q}} + \bar{\underline{K}}\underline{q} = \bar{\underline{G}}\underline{n} \tag{32}$$

where

$$\underline{q} = \begin{pmatrix} \bar{\theta}_f \\ \bar{\theta}_r \\ \bar{X}_n \\ \bar{\psi} \end{pmatrix} \tag{33}$$

and the 4 X 4 non-dimensional matrices $\bar{\underline{M}}$, $\bar{\underline{C}}$, $\bar{\underline{K}}$, and $\bar{\underline{G}}$ are as defined in Appendix C.3. These equations can also be written in first order form, as indicated in equations 19 through 22.

PART III

SYSTEM RESPONSE AND RIDE QUALITY SIMULATION

Introduction

The major objective of the model developed herein is to make possible the prediction of the AIRTRANS vehicle ride quality and to allow investigation of the effects of various parametric changes upon the ride quality as well as the effects of ride quality specifications upon system costs.

Since most ride quality specifications consist of limits upon the acceleration(s) of the vehicle as a function of frequency, it is convenient to consider the vehicle acceleration response in the frequency domain. Therefore frequency domain solution techniques are the most natural to use for these simulations. Since this approach relies upon linear system theory, the linear versions of the model are used.

System Natural Frequencies and Mode Shapes

Basic system behavior is largely characterized by the system's natural frequencies and mode shapes. Since the system under consideration is damped, normal modes* for the system do not exist in the true sense. For systems with damping which is not too severe, however, it is instructive to look at the normal modes of a system which is identical to the system under study except that all damping terms have been set to zero. Such a system will have roughly the same magnitudes of vibration associated with corresponding modes and provides insight into system behavior without the complication of the coupling due to damping. Beginning with the matrix equation (18) or (30) and setting the damping matrix $\underline{C} = 0$ and the input $\underline{u} = 0$ results in

$$\underline{M}\ddot{\underline{x}} + \underline{K}\underline{x} = 0 \tag{34}$$

---

*Normal modes in theory generally only exist for undamped systems. When a system is damped, that damping usually provides coupling between modes, allowing energy transmission between modes. The modes are therefore not "normal" or orthogonal in the mathematical sense.

Assuming a periodic solution,

$$\ddot{\underline{X}} = -w^2\underline{X} \tag{35}$$

where w^2 is the square of the undamped system natural frequency, results in

$$\begin{aligned} &(-w^2\underline{M} + \underline{K})\underline{X} = 0 \\ \text{or} \quad &(-w^2\underline{I} + \underline{D})\underline{X} = 0 \end{aligned} \tag{36}$$

where $D = M^{-1}K$ is the dynamical matrix. Equation (36) represents a classical eigenvalue problem, where the values of w^2 which satisfy (36) are the eigenvalues of the matrix D and where the vectors $\underline{X}$ which satisfy (36) are the eigenvectors of D. The square roots of the eigenvalues of D are therefore the undamped system natural frequencies, whereas the eigenvectors of D are the undamped system normal modes. In the following, the terms "undamped natural frequencies" and "mode shapes" refer to quantities calculated as just described.

When examining the system mode shapes, it is also advantageous to use the mode shapes corresponding to normalized system variables listed in Table 2 and represented in the non-dimensional equations (25) and (32). This allows direct comparisons between corresponding terms in the mode shapes.

The non-dimensional parameters and normalization factors corresponding to the dimensional parameters listed in Table 1 are listed in Table 4. For these values of system parameters, the undamped natural frequencies and normalized mode shape for the six-degree-of-freedom and four-degree-of-freedom models are listed in Tables 5 and 6 respectively. The first of the six system modes represented in Table 5 consists of a 1.6 hertz mode in which lateral body motion dominates, with fairly large motions of the wheels. The wheel motion associated with this mode is characterized by both front and rear wheels rotating in phase with each other but out of phase with the vehicle body motion, i.e.,the direction of the wheels at any one time would tend to steer the vehicle in a direction opposite to its displacement at that time. The second mode is a 2.0 hertz mode dominated by vehicle yaw motions. The wheel motion for this mode is also fairly large, with the front and rear wheels out of phase with each other and out of phase with the vehicle

TABLE 4 NOMINAL VALUES OF NON-DIMENSIONAL PARAMETERS AND NORMALIZATION FACTORS FOR AIRTRANS VEHICLE AT FULL SPEED

Parameter	Normalization Factor
$\bar{K}_3 = 100$	$x^* = 1.28$ in.
$\bar{K}_4 = 0.75$	$w^* = 17.4$ rad./sec.
$\bar{d}_1 = 1.27$	
$\bar{r} = 0.094$	
$\bar{I}_w = 3.82$	
$\bar{I} = 2340$	
$\bar{B}_w = 0.814$	
$\bar{M} = 28.4$	
$\bar{C} = 228$	
$\bar{C}_t = 8.86$	
$\bar{V} = 0.20$	
$\bar{n} = 0.35$	

TABLE 5 UNDAMPED NATURAL FREQUENCIES AND NORMALIZED MODE SHAPES, SIX-DEGREE-OF-FREEDOM MODEL

$$\underline{u} = \begin{Bmatrix} \bar{X}_f \\ \bar{X}_r \\ \bar{\theta}_f \\ \bar{\theta}_r \\ \bar{X}_m \\ \bar{\psi} \end{Bmatrix} = \begin{Bmatrix} \text{Front guidebar lateral motion} \\ \text{Rear guidebar lateral motion} \\ \text{Front wheel rotation} \\ \text{Rear wheel rotation} \\ \text{Vehicle body lateral motion} \\ \text{Vehicle body yaw rotation} \end{Bmatrix}$$

$\bar{w}_1 = 0.585$

$(f_1 = w_1(\frac{w^*}{2\pi}) = 1.62 \text{ hertz})$ $\underline{u}_1 = \begin{Bmatrix} 0.14 \\ 0.35 \\ -0.62 \\ -0.52 \\ 1.0 \\ 0.08 \end{Bmatrix}$ Lateral body displacement mode

$\bar{w}_2 = 0.711$

$(f_2 = 1.96 \text{ hertz})$ $\underline{u}_2 = \begin{Bmatrix} -0.35 \\ 0.35 \\ -0.61 \\ 0.61 \\ 0.00 \\ 1.00 \end{Bmatrix}$ Yaw mode

TABLE 5. (Continued)

$f_3 = 1.46$ (4.05 hertz)

$\bar{w}_3 = 1.46$

($f_3 = 4.04$ hertz)

$$\underline{u}_3 = \begin{pmatrix} 0.66 \\ -.66 \\ 1.00 \\ -1.00 \\ 0.00 \\ -.34 \end{pmatrix}$$

Out of phase wheel mode with some out of phase yaw*

$\bar{w}_4 = 1.51$

($f_4 = 4.18$ hertz)

$$\underline{u}_4 = \begin{pmatrix} 0.78 \\ 0.78 \\ 1.00 \\ 1.00 \\ -0.24 \\ 0.0005 \end{pmatrix}$$

In phase wheel mode with some out of phase lateral motion*

$f_5 = 6.43$ (17.82 hertz)

$\bar{w}_5 = 6.43$

($f_5 = 17.8$ hertz)

$$\underline{u}_5 = \begin{pmatrix} -0.46 \\ 0.07 \\ 1.00 \\ -0.16 \\ 0.008 \\ 0.016 \end{pmatrix}$$

Steering link resonance mode*

$\bar{w}_6 = 6.45$

($f_6 = 17.9$ hertz)

$$\underline{u}_6 = \begin{pmatrix} 0.46 \\ -0.46 \\ -1.00 \\ 1.00 \\ 0.00 \\ -0.016 \end{pmatrix}$$

Steering link resonance mode*

*Since modes three and four have (almost) the same frequency, their mode shapes are not independent, and any linear combination of the mode shapes listed is also a mode shape. The same is also true of modes five and six.

TABLE 6 UNDAMPED NATURAL FREQUENCIES AND NORMALIZED MODE SHAPES, FOUR-DEGREE-OF-FREEDOM MODEL

$$\underline{u} = \begin{pmatrix} \bar{\theta}_f \\ \bar{\theta}_r \\ \bar{X}_m \\ \bar{\psi} \end{pmatrix} = \begin{matrix} \text{Front wheel rotation} \\ \text{Rear wheel rotation} \\ \text{Vehicle body lateral motion} \\ \text{Vehicle body yaw rotation} \end{matrix}$$

$\bar{w}_1 = 0.601$

$(f_1 = \bar{w}_1(\frac{w^*}{2\pi}) = 1.66$ hz)

$$\underline{u}_1 = \begin{pmatrix} -0.65 \\ -0.55 \\ 1.00 \\ 0.08 \end{pmatrix}$$

Lateral body displacement mode

$\bar{w}_2 = 0.725$

$(f_2 = 2.00$ hz)

$$\underline{u}_2 = \begin{pmatrix} -0.63 \\ 0.63 \\ 0.00 \\ 1.00 \end{pmatrix}$$

Yaw mode

$\bar{w}_3 = 1.46$

$(f_3 = 4.05$ hz)

$$\underline{u}_3 = \begin{pmatrix} 1.00 \\ -1.00 \\ 0.00 \\ -0.34 \end{pmatrix}$$

Out-of-phase wheel mode

$\bar{w}_4 = 1.51$

$(f_4 = 4.18$ hz)

$$\underline{u}_4 = \begin{pmatrix} 1.00 \\ 1.00 \\ -0.24 \\ 0.00 \end{pmatrix}$$

In-phase wheel mode

yaw motions. The third and fourth modes are at practically the same frequency (4.1-4.2 hertz) and are modes dominated by wheel motions with some body displacement and yaw. Since these two modes are at practically the same frequency, they are (nearly) indistinguishable,and any linear combination of the two mode shapes listed is also (nearly) a mode shape. They have been listed as an out-of-phase wheel mode and an in-phase wheel mode. Modes five and six are also of approximately the same frequency and represent resonances of the guidebar steering links. The motion associated with these modes is primarily motion of the wheels and guidebars, the motion of each wheel assembly (front or rear) being out of phase with the corresponding guidebar assembly (front or rear).

When the effects of damping on the system are taken into account, the frequencies of the modes described above are changed somewhat, and some coupling is introduced between modes. These effects are relatively small, however, and the same general behavior is expected. The eigenvalues of the damped system are found by determining the eigenvalues of the matrix A defined in equation (21). The damped natural frequencies and critical damping ratio for each complex conjugate pair of system eigenvalues are tabulated in Table 7. The damped natural frequency is here defined as the magnitude of the imaginary part(s) of the corresponding complex conjugate pair of system eigenvalues, and the damping ratio is defined as the ratio of the absolute value of the real part(s) to the magnitude(s). Comparing the damped frequencies from Table 7 with the undamped frequencies in Tables 5 and 6, it is noted that the damped frequencies differ somewhat from the undamped natural frequencies, with the effect of damping being greatest in the lower frequency modes.

System Transfer Functions

Since it is convenient to use the frequency domain for ride quality investigation, the system transfer functions are of primary interest. There are found by substituting $\dot{\underline{x}} = jw\underline{x}$ into equation 19, yielding

$$jw\underline{x} = \underline{A}\underline{x} + \underline{B}\underline{u} \tag{37}$$

or

$$(jw\underline{I}-\underline{A})\underline{x} = \underline{B}\underline{u}$$

Solving for x,

$$\underline{x} = (jw\underline{I}-\underline{A})^{-1}\underline{B}\underline{u}$$

$$= -(w^2\underline{I}+\underline{A}^2)^{-1}(jw\underline{I}+\underline{A})\underline{B}\underline{u} \tag{38}$$

TABLE 7 DAMPED NATURAL FREQUENCIES AND DAMPING RATIOS

Mode	Six-Degree-of-Freedom Model			Four-Degree-of-Freedom Model		
	$\bar{w}_d$(rad/sec)	f_d(hz)	ζ	$\bar{w}_d$(rad/sec)	f_d(hz)	ζ
1	0.557	1.54	0.38	0.571	1.58	0.39
2	0.695	1.93	0.42	0.710	1.97	0.43
3	1.34	3.72	0.16	1.33	3.68	0.16
4	1.46	4.02	0.11	1.45	4.02	0.17
5	6.43	17.8	0.009	-	-	-
6	6.45	17.9	0.007	-	-	-

Definitions: $\bar{w}_d$ = non-dimensional damped frequency

$f_d = \bar{w}_d(\frac{w^*}{2\pi})$ = damped frequency in hertz

ζ = damping ratio

$w^* = 17.4$ rad/sec. $f^* = w^*/2\pi = 2.77$ hz.

The later form of (38) is used for computational purposes since the matrix which requires inversion is real valued. The output of interest is the acceleration at the passenger location of interest and can be written

$$\begin{aligned} y &= \ddot{X}_m + \ell\ddot{\psi} \\ &= \underline{d}^T\ddot{\underline{x}} = \underline{d}^T(jw)\underline{x} \end{aligned} \tag{39}$$

where

$$\underline{d}^T = [0\ 0\ 0\ 0\ 0\ 0\ 0\ 0\ 0\ 0\ 1\ \ell]$$

for the six-degree-of-freedom model and $\underline{d}^T = [0\ 0\ 0\ 0\ 0\ 0\ 1\ \ell]$ for the four-degree-of-freedom model and where ℓ is the position of the passenger location ahead of the mass center of the vehicle.

Substituting (38) into (39),

$$\begin{aligned} y &= -\underline{d}^T(jw)(w^2\underline{I}+\underline{A}^2)^{-1}(jw\underline{I}+\underline{A})\underline{B}\underline{u} \\ &= \underline{d}^T(w^2\underline{I}+\underline{A})^{-1}(w^2\underline{I}+\underline{A}^2)^{-1}(w^2\underline{I}-jw\underline{A})\underline{B}\underline{u} \\ &= \underline{g}^T(jw)\underline{u} \end{aligned} \tag{40}$$

where

$$\underline{g}^T(jw) = \underline{d}^T(w^2I+A^2)^{-1}(w^2I-jwA)\underline{B}$$

is a row vector of transfer functions relating each of the inputs and the output. Since there are four inputs, $\underline{g}^T(jw)$ has four individual terms, and (40) expanded takes the form

$$y = [G_1\ G_2\ G_3\ G_4] \begin{Bmatrix} u_1 \\ u_2 \\ u_3 \\ u_4 \end{Bmatrix} \tag{41}$$

where, it is recalled, that u_1 and u_2 are left and right front guidewheel displacements, respectively, and u_3 and u_4 are left and right rear guidewheel displacements, respectively. Because the vehicle is symmetrical, the effect on the output of a right front (or rear) guidewheel displacement is identical to the effect of a left front (or rear) guidewheel displacement.

This being the case, the terms G_1 and G_2 are identical, as are the terms G_3 and G_4, so that

$$y = [\, G_1 \; G_1 \; G_3 \; G_3]\underline{u} \tag{42}$$

Additionally, it is noted that if the passenger location of interest is at the vehicle center, i.e.,if $\ell = 0$, $G_3 = -G_1$ because the vehicle is antisymmetric about the centerline between the front and back.

Using the six-degree-of-freedom model with parameters as defined in Table 1, the magnitudes of the transfer functions G_1 and G_3 are plotted in Figure 6 for a passenger location at the vehicle center (ℓ=0) and for a passenger location 48 inches ahead (ℓ=48 in.) of the vehicle center.

Further combination of the transfer functions above is accomplished by noting the relationship between front and rear inputs. Assuming that the input to the rear guidewheel on either side of the vehicle is just the input to the front guidewheel on the same side delayed for the period of time it takes the vehicle to travel the distance between the guidewheel,

$$u_3 = u_1 \, e^{-jw(\frac{2d_2}{V})} \tag{43}$$

$$u_4 = u_2 \, e^{-jw(\frac{2d_2}{V})} \tag{44}$$

where $(\frac{2d_1}{V})$ is the time delay between guidewheels. Substituting (43) and (44) into (42),

$$y = [G_1 \; G_1 \; G_3 \; G_3] \begin{Bmatrix} u_1 \\ u_2 \\ u_1 e^{-jw(\frac{2d_2}{V}} \\ u_2 e^{-jw(\frac{2d_2}{V})} \end{Bmatrix}$$

$$= [(G_1 + G_3 e^{-jw(\frac{2d_2}{V})})(G_1 + G_3 e^{-jw(\frac{2d_2}{V})}] \begin{Bmatrix} u_1 \\ u_2 \end{Bmatrix}$$

$$= [G \; G] \begin{Bmatrix} u_1 \\ u_2 \end{Bmatrix} \tag{45}$$

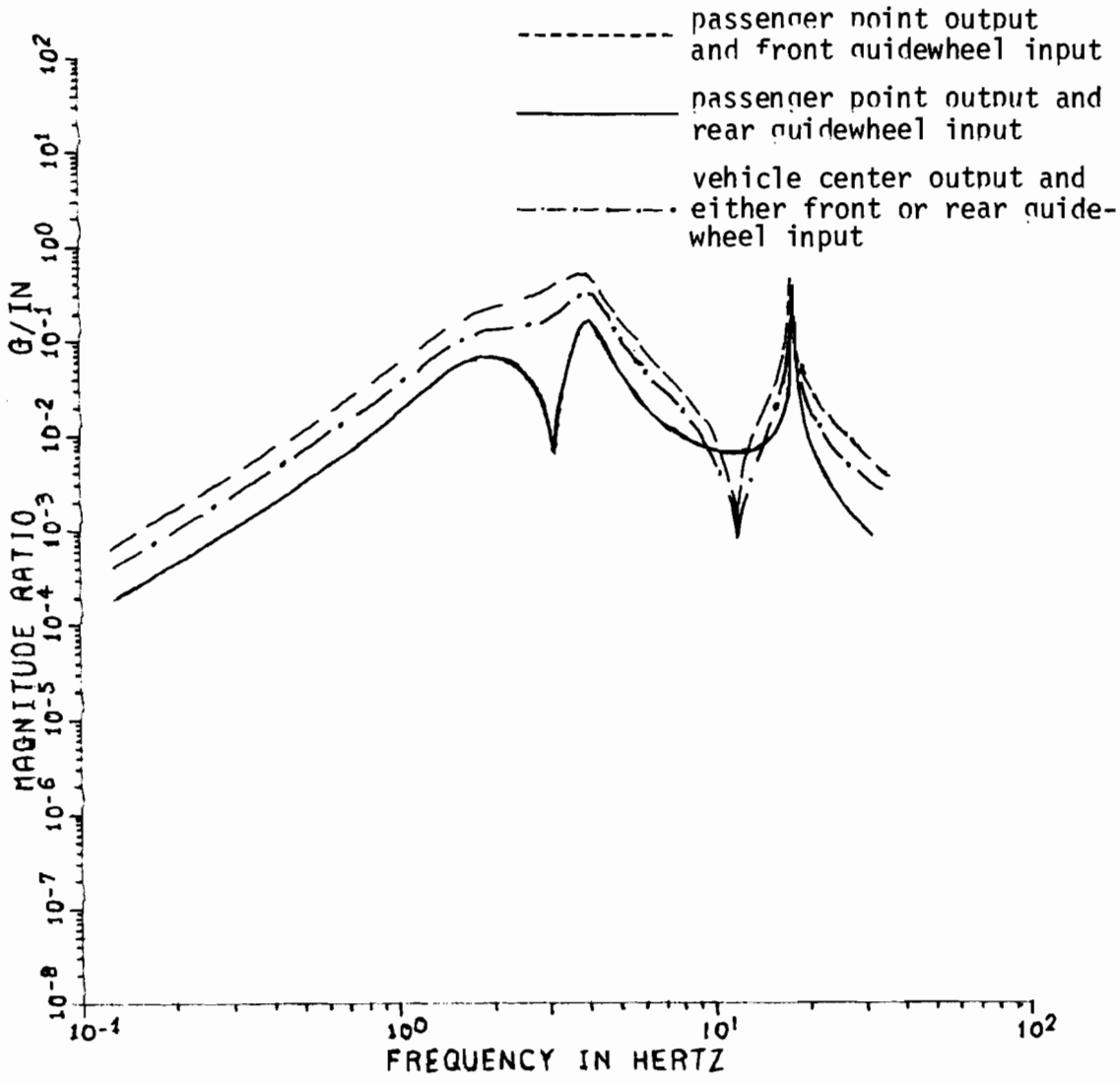

Figure 6. Transfer functions relating inputs from various guidewheels and outputs at vehicle center and a passenger point 48 in. ahead of vehicle center (six-degree-of-freedom model)

where

$$G = G_1 + G_3 e^{-jw(\frac{2d_2}{V})} \tag{46}$$

is the transfer function relating the output and the left (or right) sidewall profile, and where the rear guidewheel is assumed to follow the same profile as the front guidewheel (only delayed) on each side. This transfer function using the six-degree-of-freedom model is shown for a passenger position at the vehicle center (ℓ=0) in Figure 7 and for a passenger position 48 inches ahead of vehicle center (ℓ=48 in.) in Figure 8. It is noted that in addition to the modal resonances corresponding to the natural frequencies tabulated in Tables 5 and 6, there are multiple kinematic resonances (and anti-resonances) present. These kinematic resonances correspond to input frequencies or wavelengths which are related to the distance between the front and rear guidewheels. In examining Figure 7, the transfer function for a passenger location at the vehicle center, it is noted that the kinematic resonances correspond to frequencies for which the motion inputs to the front and rear guidewheels are in phase. The dips in the curve between peaks, or the "anti-resonances," correspond to input spatial frequencies for which the motions of the front and rear guidewheels are 180° out of phase. When this occurs, the vehicle pitch motion is excited predominantly, and there is very little motion of the vehicle center. This is further understood by noting that the transfer function for the passenger point 48 inches ahead of center (Figure 8) has kinematic resonances peaks in the same places and of about the same magnitudes as the vehicle center transfer function, but the "anti-resonant" dips are not nearly as significant since the passenger in this case is located away from the pitch center. At this location, the excited pitch motion contributes to the passenger point motion at these "anti-resonant" frequencies.

The transfer functions for the four-degree-of-freedom model with the output at the vehicle center and with the output at a passenger location 48 inches ahead of the vehicle center are shown in Figures 9 and 10, respectively. The four-degree-of-freedom transfer functions are very nearly the same as the six-degree-of-freedom transfer functions, except in the immediate vicinity of the 17 hertz guidebar resonance. Since this resonance is lightly damped, it represents a fairly sharp peak in the six-degree-of-freedom transfer function which is not represented in the four-degree-of-freedom model.

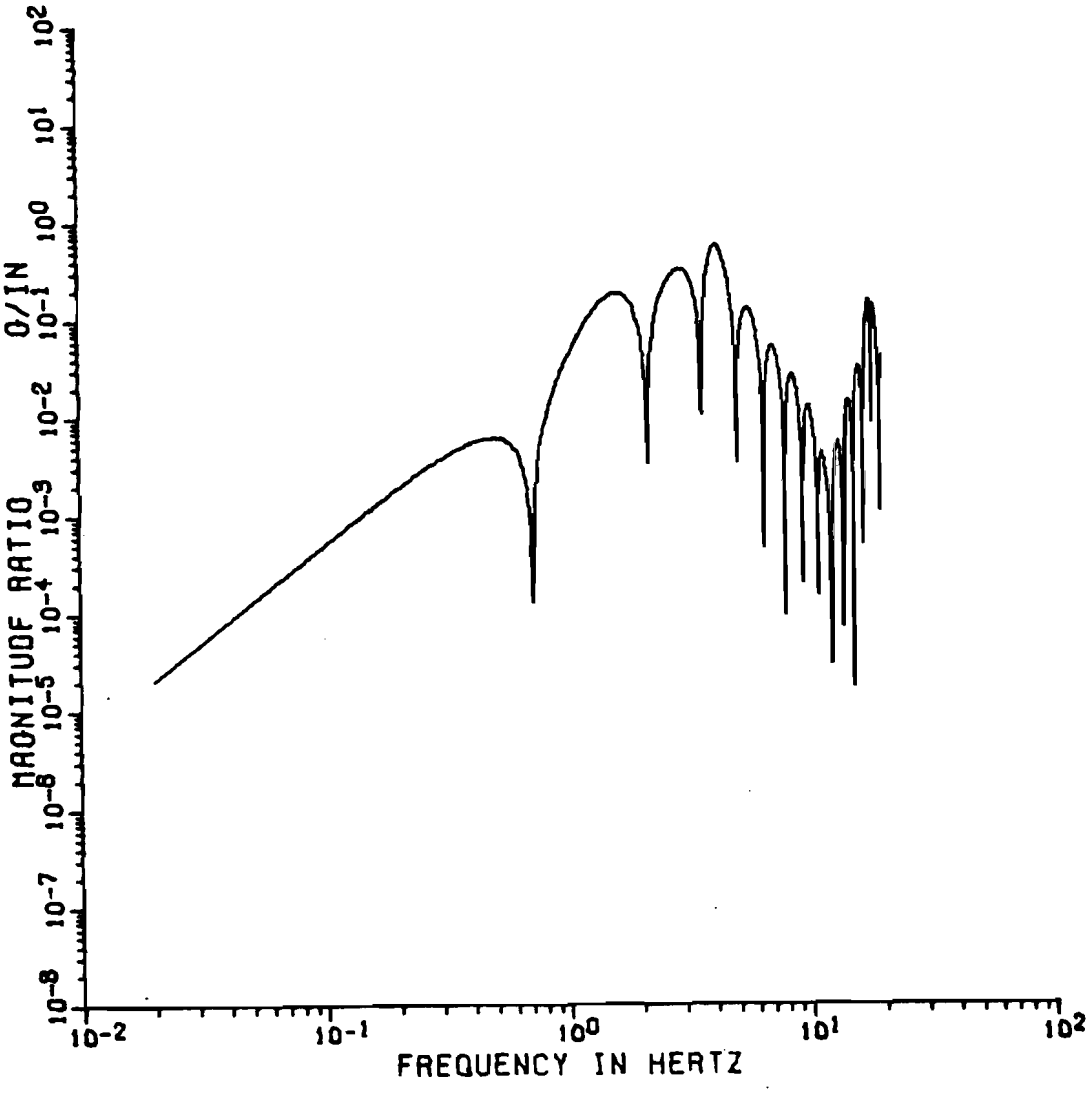

Figure 7. Magnitude ratio of the acceleration output at vehicle center with input to the left (or right) steering guide (six-degree-of-freedom model)

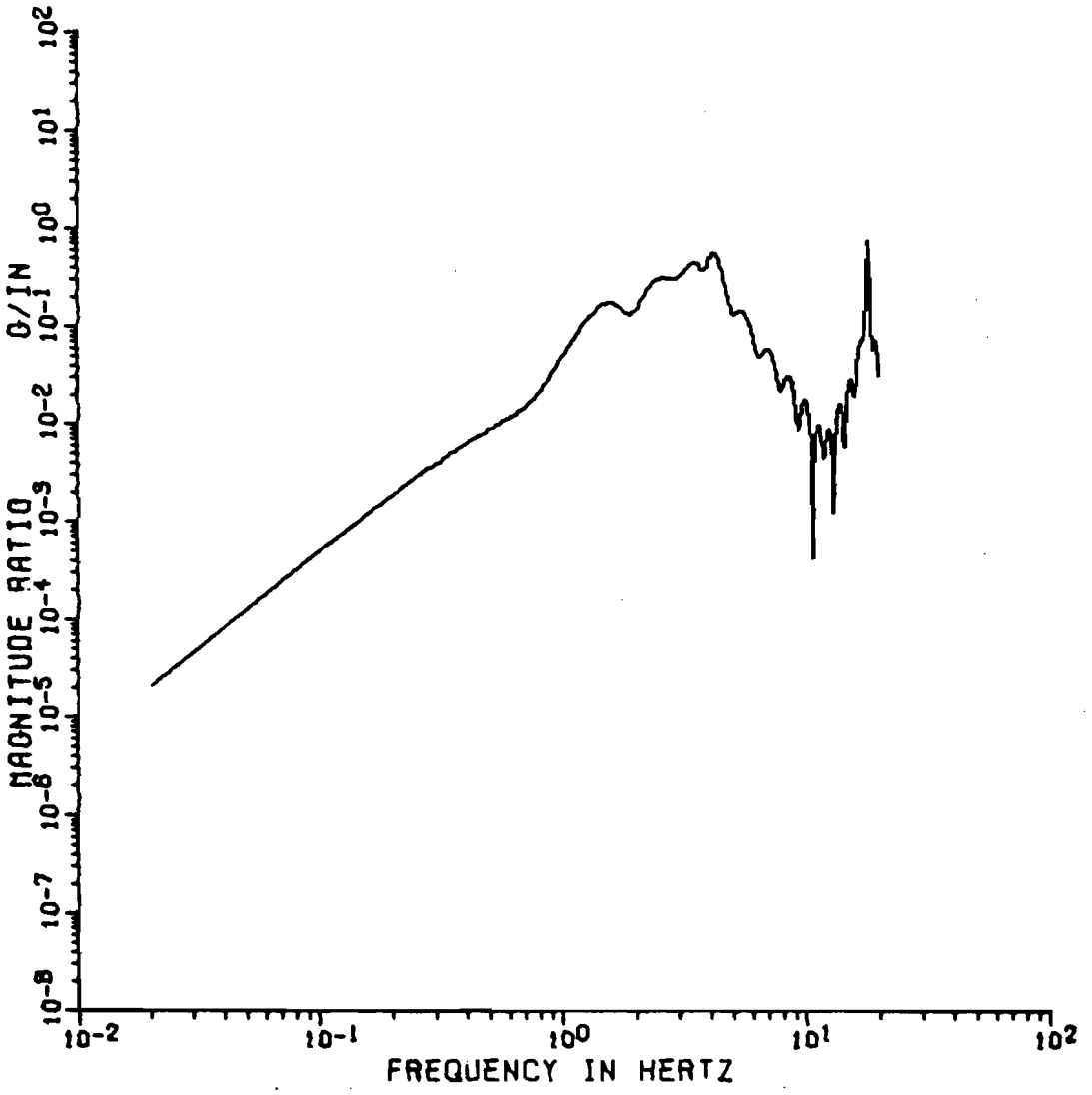

Figure 8. Magnitude ratio of the acceleration output at a passenger point with input to the left (or right) steering guide (six-degree-of-freedom model)

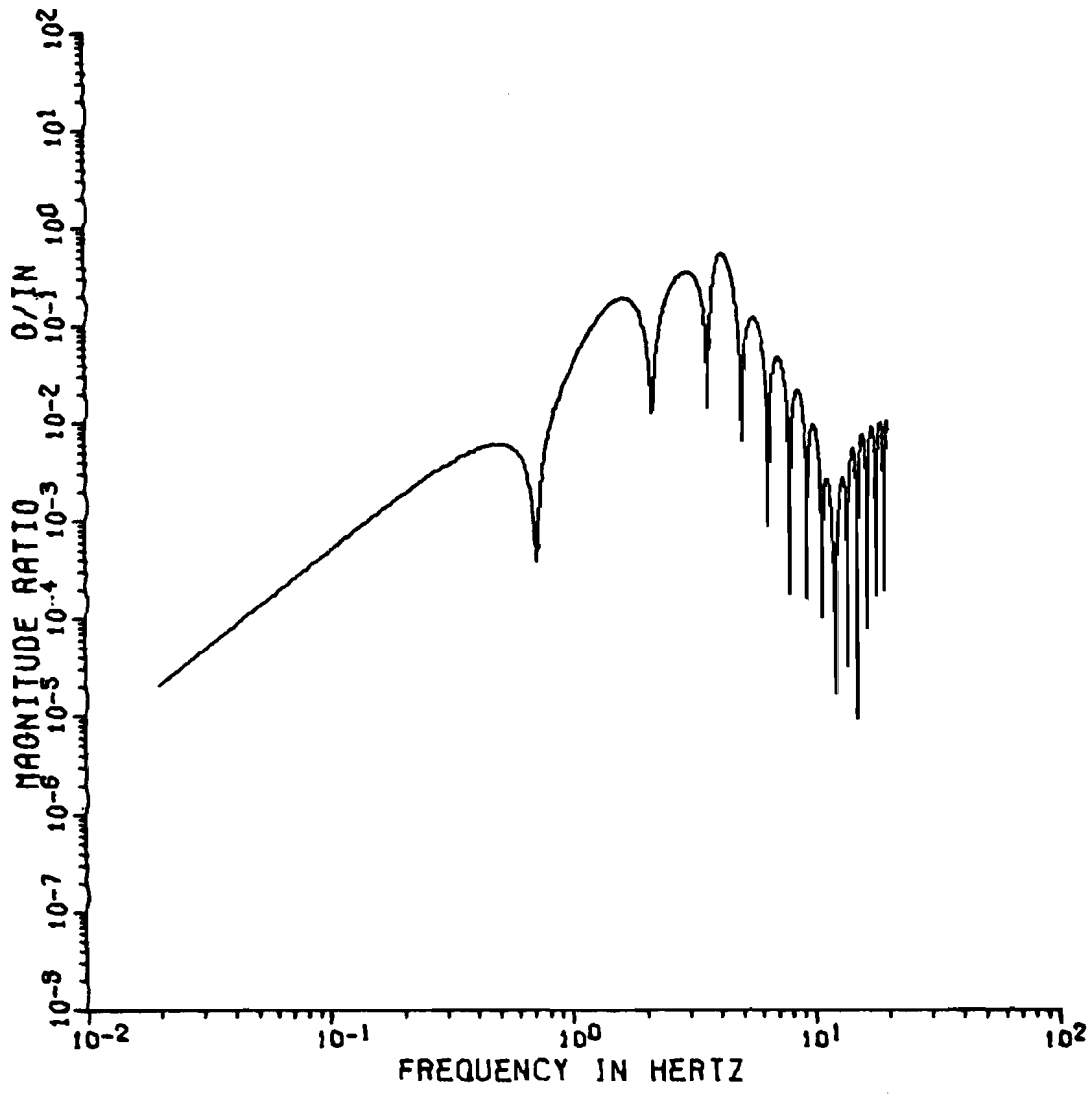

Figure 9. Magnitude ratio of the acceleration output at vehicle center with input to the left (or right) steering guidebars (four-degree-of-freedom model)

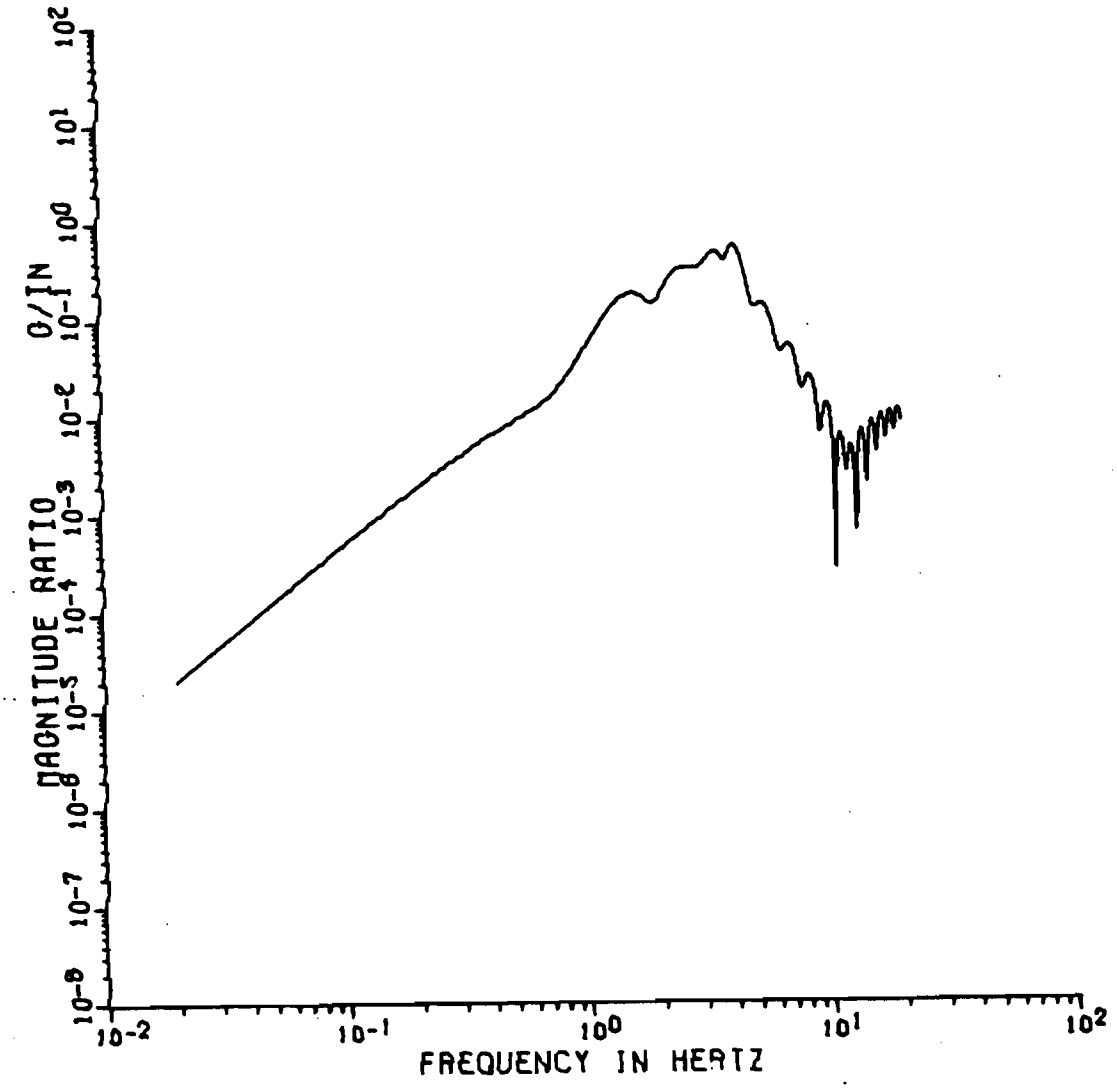

Figure 10. Magnitude ratio of the acceleration output at a passenger point 48 inches ahead of the vehicle center with input to the left (or right) steering guidebars (four-degree-of-freedom model)

Predicted Spectra of Vehicle Output

For ride quality assessment of a transportation vehicle, most criteria are based upon the vehicle acceleration spectra. Since the model which has been developed predicts only the lateral spectrum, the vehicle output of interest is the lateral acceleration spectrum at a given passenger location. Since there are two (right and left) sidewall inputs, the system is a two-input-single-output system as defined by equation (45), and the spectrum of the output is related to the spectra of the inputs by the equation

$$\begin{aligned} P_y(f) &= G(f)\, G(-f)\, P_{u_1}(f) \\ &+ G(-f)\, G(f)\, C_{u_1u_2}(f) + G(f)\, G(-f)\, C_{u_2u_1}(f) \\ &+ G(f)\, G(-f)\, P_{u_2}(f) \\ &= G(f)\, G(-f)\, [P_{u_1}(f) + C_{u_1u_2}(f) + C_{u_2u_1}(f) + P_{u_2}(f)] \\ &= |G(f)|^2 (P_{u_1}(f) + C_{u_1u_2}(f) + C_{u_2u_1}(f) + P_{u_2}(f)) \end{aligned} \tag{47}$$

where $P_{u_1}(f)$ is the autospectral density of u_1, $C_{u_1u_2}(f)$ and $C_{u_2u_1}(f)$ are the cross spectral densities of u_1 and u_2, and $P_{u_2}(f)$ is the autospectral density of u_2.

When guidewheels on both sides of the vehicle are in contact with the guideway, calculation of the output spectrum using (47) requires knowledge not only of the character of each of the sidewall profiles themselves (their autospectral densities) but also information about their relationship to each other, including phase (cross spectral densities). Luckily from a computational point of view, it has been observed that in many situations the guidewheels are in contact with only one sidewall, with the opposite guidewheels freely "floating." This is the case particularly around corners, where the vehicle is in contact with the outside wall only. (In straight sections of guideway, the vehicle effectively wanders from side to side, making contact with one side and then the other.) When this is true, the input on the side with no contact is zero, and (47) reduces to

$$P_y(f) = |G(f)|^2 P_u(f) \tag{48}$$

where $P_u(f)$ is the autospectral density of the sidewall in contact.

It has been suggested by some authors that typical guideway profile spectra for guideway floors (vertical inputs) are of the form $P(\Omega) = \frac{A}{\Omega^2}$, where Ω is the spacial frequency (inverse of the wavelength) of the guideway irregulatities and A is a constant.[4] A vehicle traveling at a velocity V therefore sees an input of the form

$$(f) = \frac{AV}{f^2} \tag{49}$$

where $f = V\Omega$ is the time-based frequency (cycles/sec.) of the input. Typical values of the constant A vary from about 10^{-7} to 10^{-3} feet, depending upon the surface roughness. Assuming that the guideway sidewall roughness is of the same form as here suggested for sidewall floor roughness, substitution into (48) yields

$$P_u(f) = |G(f)|\,(AV/f^2)$$

or

$$\left(\frac{P_y(f)}{AV}\right) = \left|\frac{G(f)}{f}\right|^2 \tag{50}$$

Figure 11 shows $P_y(f)/AV$ as represented in (50) for lateral acceleration output at the vehicle center using the six-degree-of-freedom model. Since this plot is on log-log coordinates, it is applicable to any values of the constants A and V. The form of the actual output spectra, $P_y(f)$, for differing surface roughness A and velocities V will be identical in form but shifted along the logarithmic ordinate from each other. The only restriction is that the input be of the form represented in (49). For comparison purposes, the lateral acceleration spectra measured at the vehicle center, represented as an ensemble average of data measured in 800-ft.-radius curves, is plotted also in Figure 12.[5] The level is adjusted so that the levels of the two curves

---

[4] See, for example, H. H. Richardson, et al, "Dynamics of Simple Air-Supported Vehicles Operating over Irregular Guideways," Report DSR 76110-4, Massachusetts Institute of Technology, Clearinghouse No. PB 173655, June 1967, p. 9.

[5] Healey, A. J., "Ride Quality Assessment for the AIRTRANS System," Report No. MEUT-1, under contract no. DOT-OS-50126, Mechanical Engineering Department, The University of Texas at Austin, 1976.

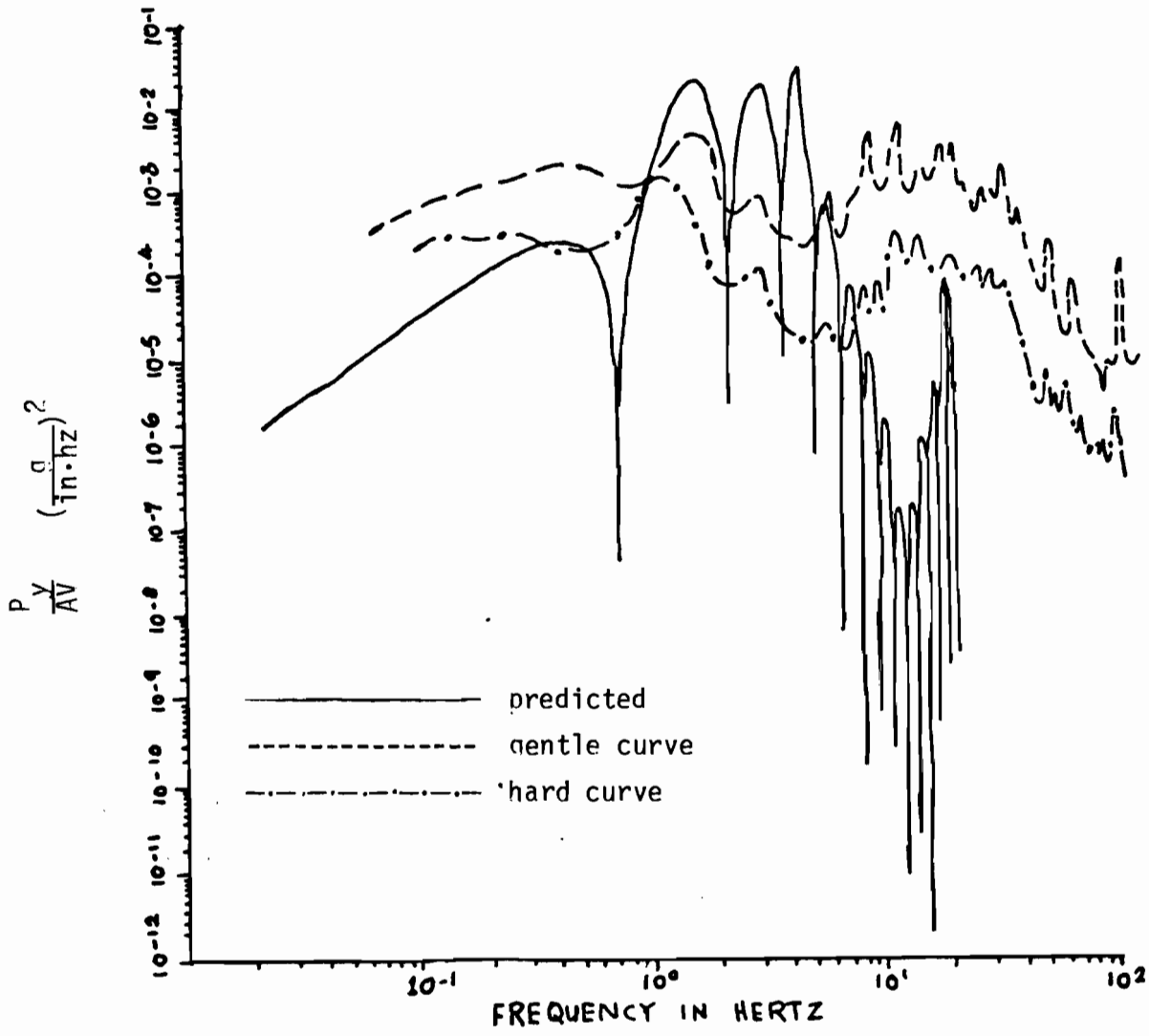

Figure 11. Normalized autospectral density of the predicted acceleration output using input spectrum of the form $P_u(f) = \frac{AV}{f^2}$ compared with measured spectra in gentle (800-ft.-radius) and hard (150-ft.-radius) curves

correspond at the frequency f = 1.0 hertz. This would correspond to a value of AV = 1.4 in^2 hz, or, since V = 25 ft/sec, A = 5.7 x 10^{-4} in^2/ft = 4.0 x 10^{-6} ft.

Murray and Smith have shown that a more accurate representation of the guideway sidewall roughness for the AIRTRANS guideway is of the form

$$P_u(\Omega) = \frac{K}{\Omega^{2.8}} \tag{51}$$

where K is a constant depending upon the roughness level and Ω is again the spacial frequency.[6] Converting to the form of a function as "seen" in time by a vehicle moving at a velocity V,

$$P_u(f) = \frac{K \cdot V^{1.8}}{f^{2.8}} \tag{52}$$

where f is the time based frequency (hertz). Substituting (52) into (48)

$$P_y(f) = KV^{1.8} \frac{|G(f)|^2}{f^{2.8}} \tag{53}$$

or

$$\frac{P_y(f)}{KV^{1.8}} = \frac{|G(f)|^2}{f^{2.8}} \tag{54}$$

Figure 12 shows ($Py(f)/KV^{1.8}$) from (52) for a passenger point at the vehicle center. Letting V = 25 ft/sec and K = 5.7 x 10^{-5} $in^2/ft^{1.8}$ for 800 ft. radius curves and K = 1.2 x 10^{-4} $in^2/ft^{1.8}$ for 150-ft.-radius curves as given by Murray, measured lateral acceleration spectrum is converted to the form $P_y(f)/KV^{1.8}$ and also plotted in Figure 13.[7] As can be seen from the figure, the predicted spectrum agrees reasonably well with the measured spectrum in the lower frequency (below about 8 hz) range. The measured spectrum shows definite peaks corresponding to the kinematic resonances, however the peaks are not nearly as sharp as those in the predicted data. Additionally the "anti-resonances" in the measured data are much shallower. These effects

---

[6] W. R. Murray and C. C. Smith, "Guideway Sidewall Roughness and Guidewheel Spring Compressions of the Dallas/Fort Worth Airtrans," Research Report RR-42, Council for Advanced Transportation Studies, The University of Texas at Austin, 1976.

[7] Ibid, p. 37.

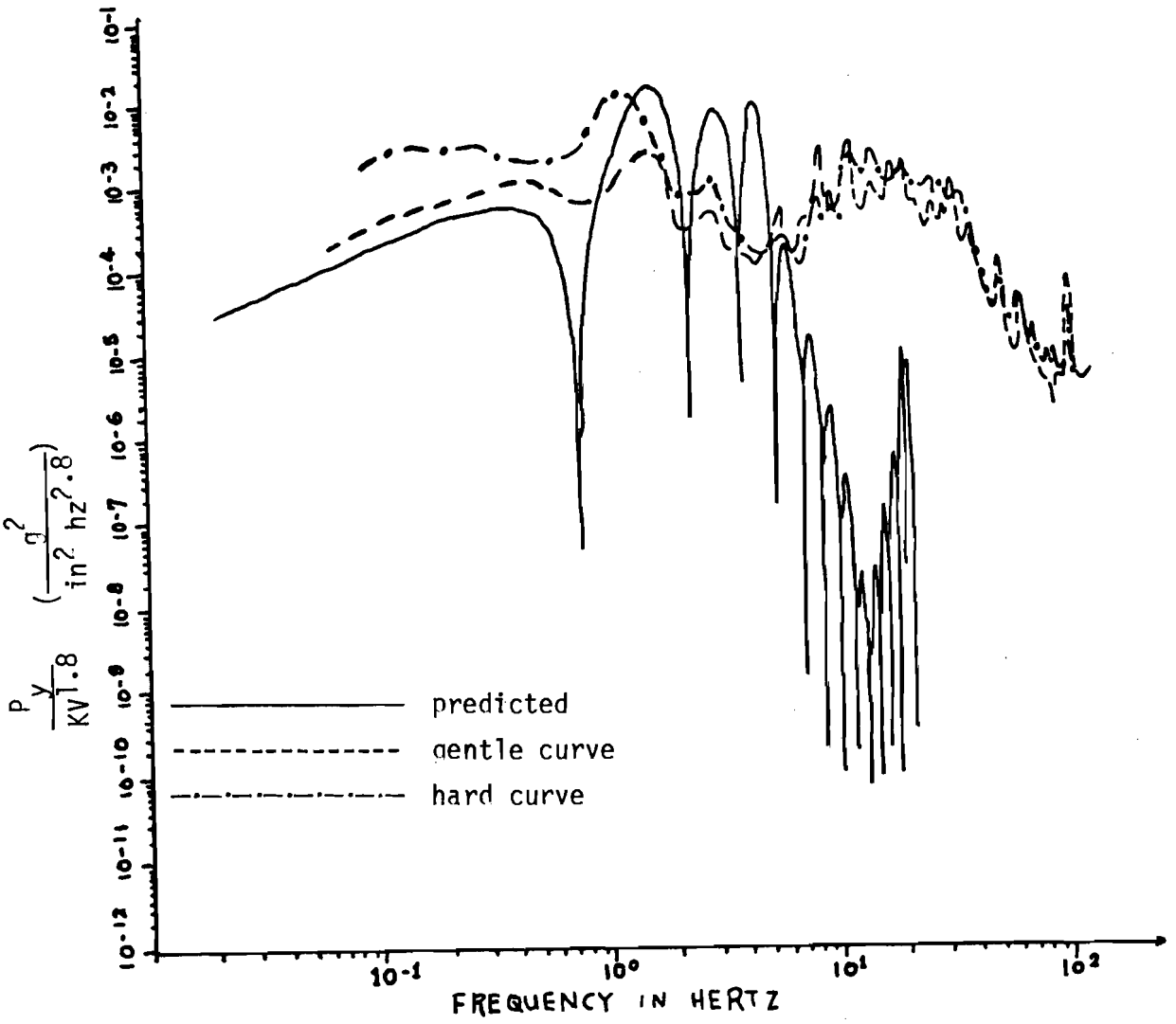

Figure 12. Normalized autospectral density of the predicted acceleration output using input spectrum of the form $P_u(f) = \frac{KV^{1.8}}{f^{2.8}}$ (after Murray) compared with measured spectra in gentle (800-ft.-radius) and hard (150-ft.-radius) curves

are to be expected, since non-rigid body effects in the actual vehicle and the resolution limitations of the measurement instrumentation and data processing would tend to "flatten" the measured data relation to the predicted data.

In the higher frequency region (above 8 hz.) the measured spectra are much higher in level than the predicted spectrum. This is to be expected since many effects not included in the model have appreciable effects in this region. Onboard compressor vibrations, vibrations due to wheel and driveline unbalances, panel resonances, and vehicle body bending modes are a few of the things which may contribute to the measured spectra in this region but would be extremely cumbersome to include in the model.

Response Sensitivity to Changes in Parameters

In examination of the vehicle model, it is instructive to investigate the effect upon ride quality of changing the basic vehicle parameters. To do this, a limited sensitivity study was undertaken considering the seven basic non-dimensional parameters listed in Table 8. In this study, the predicted output spectra subject to an input spectra of the form $P_u(f) = AV/f^2$ was used, although the general trends are applicable to other forms of input. Using the parameters previously used as representative of the present AIRTRANS vehicle as a base case, each of the parameters in Table 8 were varied individually to values lower and higher than its nominal value while holding all other variables constant at their nominal values. The effects upon the output spectra for each case are shown in Figures 13-19. As can be seen from the figures, changes in the damping ratio $\bar{B}_w$ (Figure 13) had almost no effect. Changes in the coupling stiffness ratio $\bar{K}_4$ (Figure 14), the cornering coefficient ratio $\bar{C}$ (Figure 15), and the torque coefficient ratio $\bar{C}_t$ (Figure 16), had relatively small effects upon the spectra and, hence, the ride quality. The parameters in which changes most effect the output spectra include the steering link radius ratio $\bar{r}$ (Figure 17), the steering lever ratio n (Figure 18), and the velocity ratio $\bar{V}$ (Figure 19). Both $\bar{r}$ and n affect the steering gain, which apparently is the critical effect. The most effecitve methods of changing the ride quality by vehicle parametric changes therefore include the steering gain and the vehicle velocity.

TABLE 8 SENSITIVITY ANALYSIS OF THE POWER SPECTRAL DENSITY OF THE ACCELERATION OUTPUT TO CHANGES IN THE NON-DIMENSIONAL PARAMETERS

Non-Dimensional Parameter	Nominal Value	Perturbed Values Used in Sensitivity Study	
$\bar{K}_4$	0.75	0.5	2
$\bar{r}$	.094	0.04	0.15
η	0.35	0.25	0.6
$\bar{B}_w$	0.814	0.573	1.07
$\bar{c}$	228	172	287
$\bar{C}_t$	8.86	5.73	13.4
$\bar{V}$	0.203	0.1	0.6

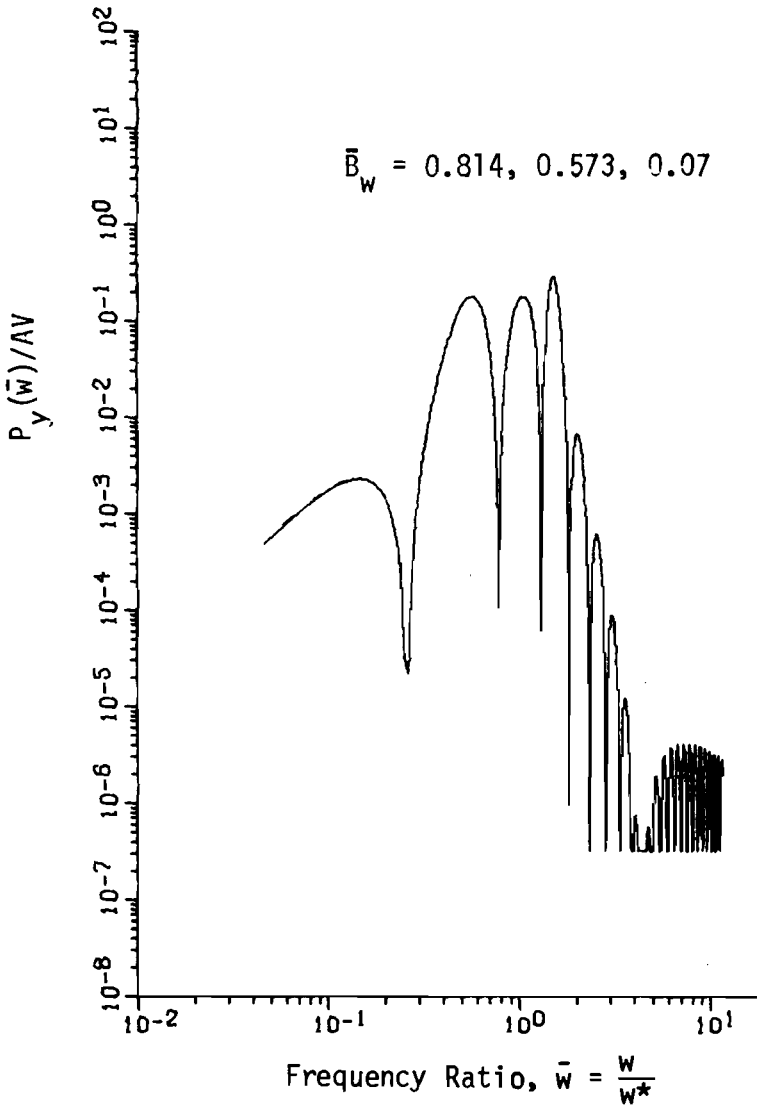

Figure 13. Normalized autospectral density of the output at vehicle center with AV/f^2 input spectra for various values of $\bar{B}_w$.

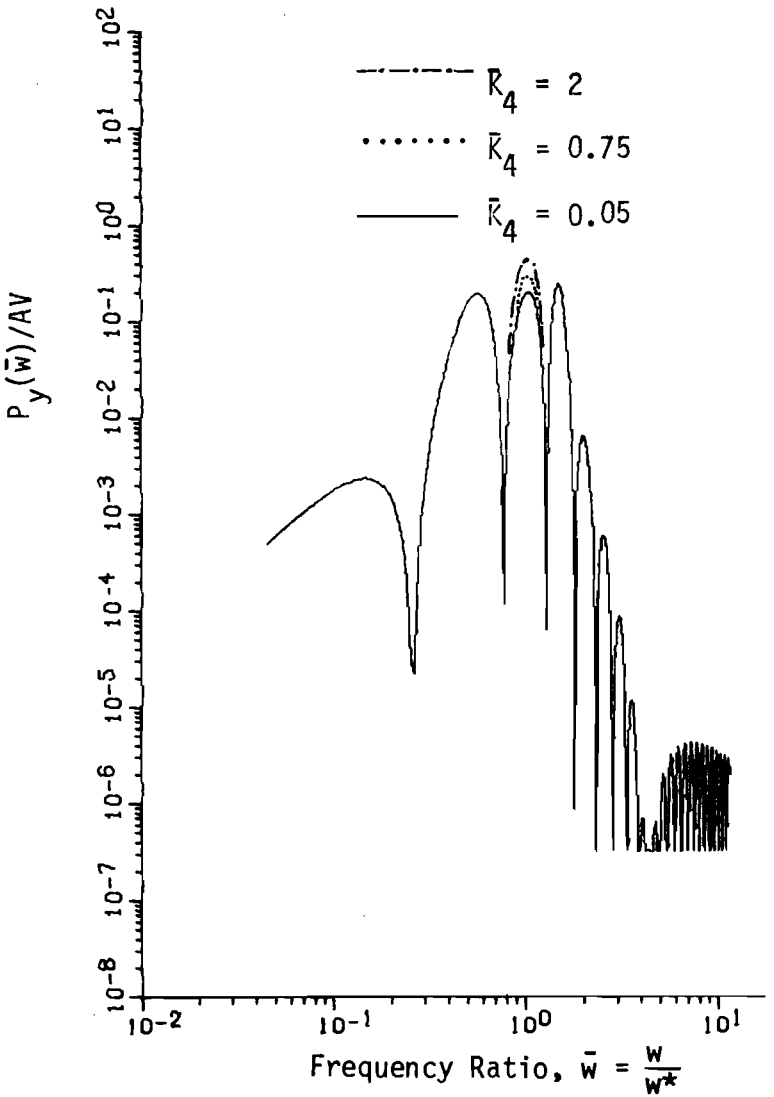

Figure 14. Normalized autospectral density of the output at vehicle center with AV/f^2 input spectra for various values of $\bar{K}_4$.

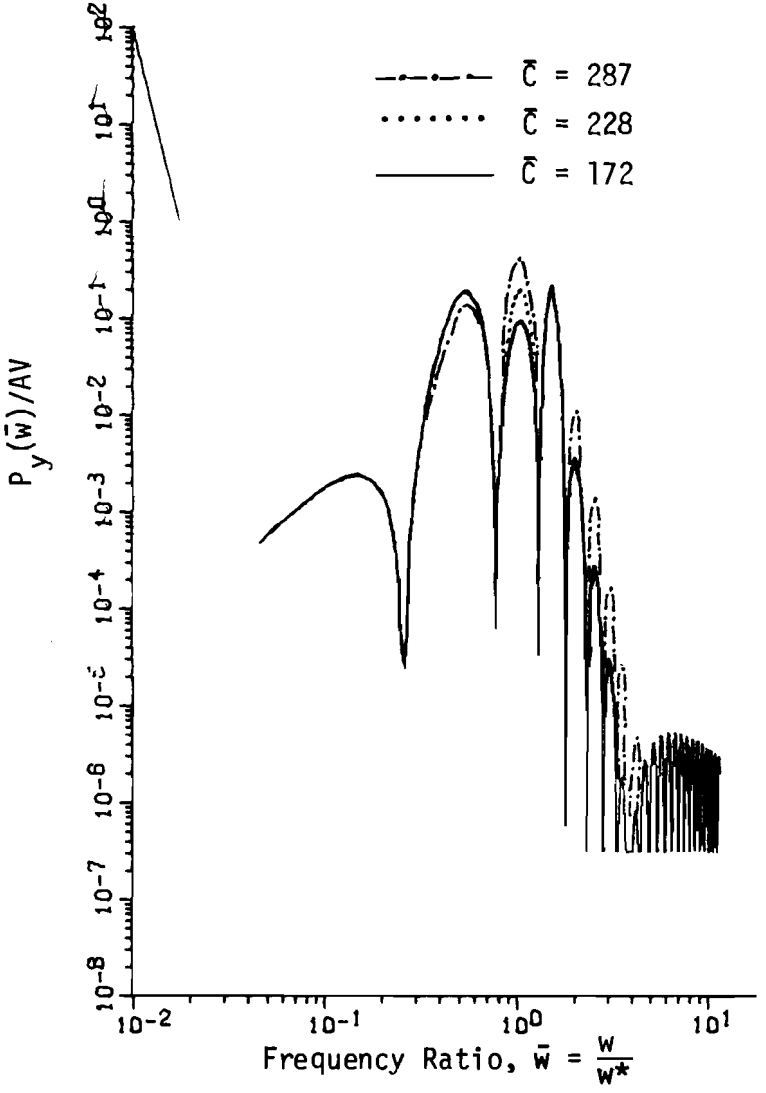

Figure 15. Normalized autospectral density of the output at vehicle center with AV/f^2 input spectra for various values of $\bar{C}$.

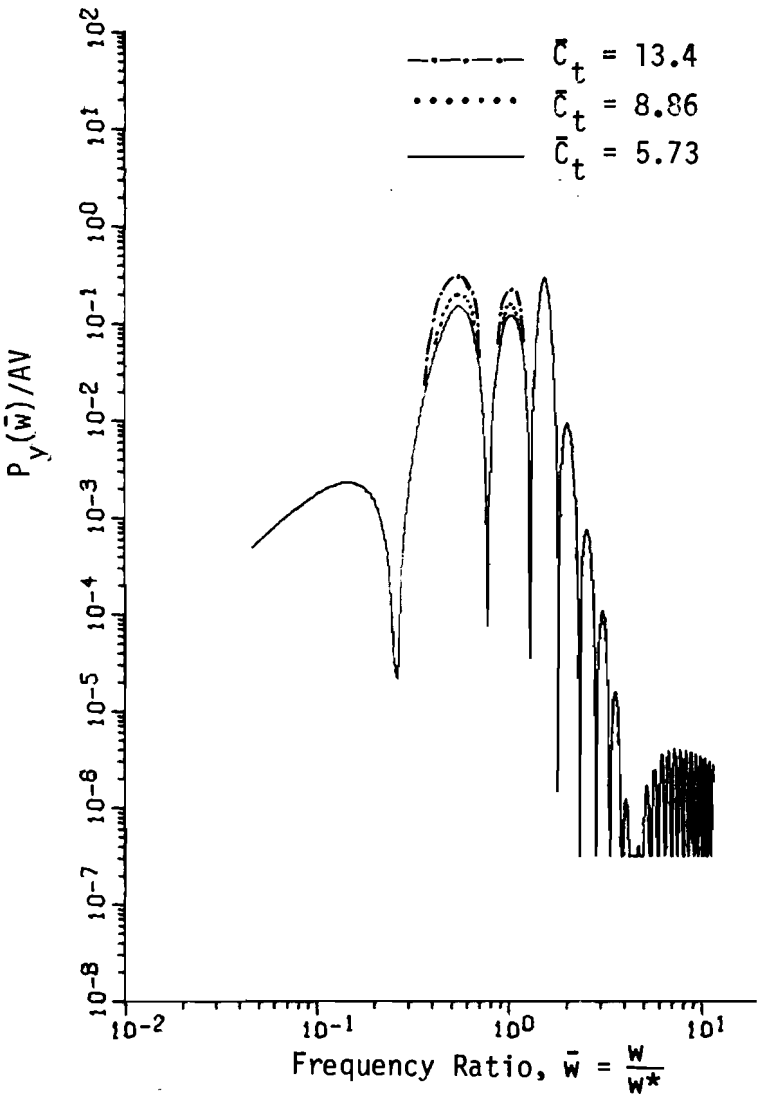

Figure 16. Normalized autospectral density of the output at vehicle center with AV/f^2 input spectra for various values of $\bar{C}_t$.

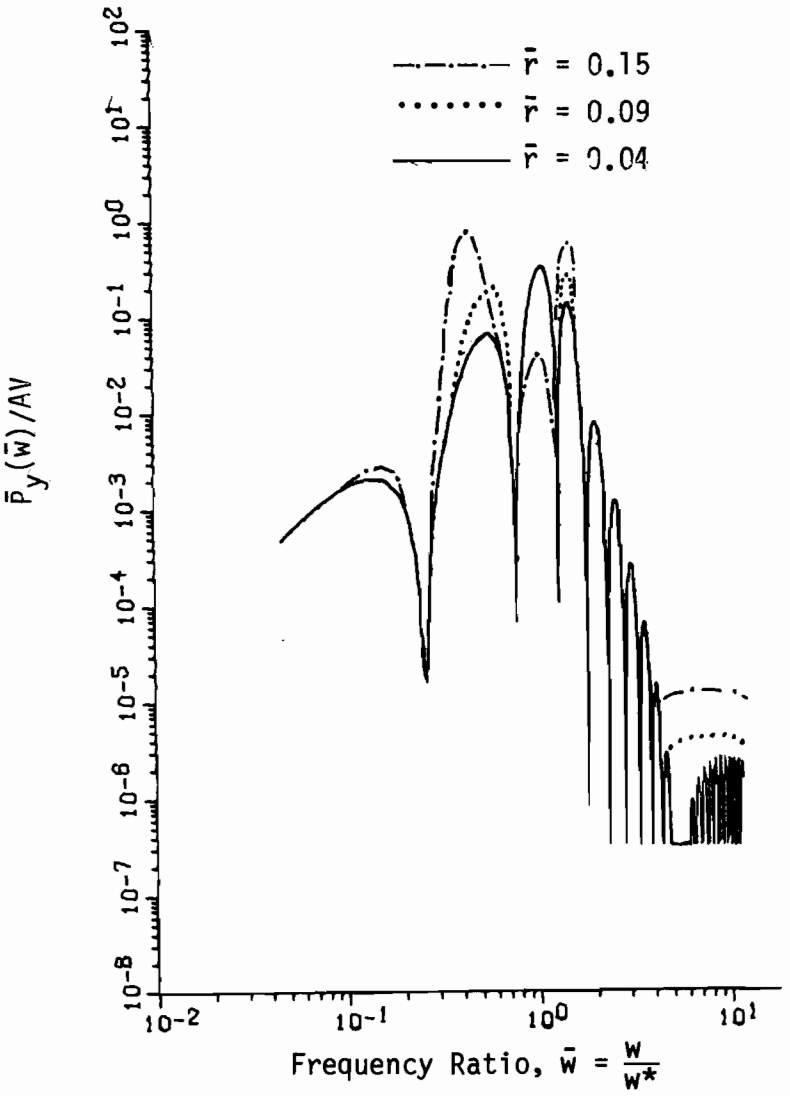

Figure 17. Normalized autospectral density of the output at vehicle center with AV/f^2 input spectra for various values of $\bar{r}$.

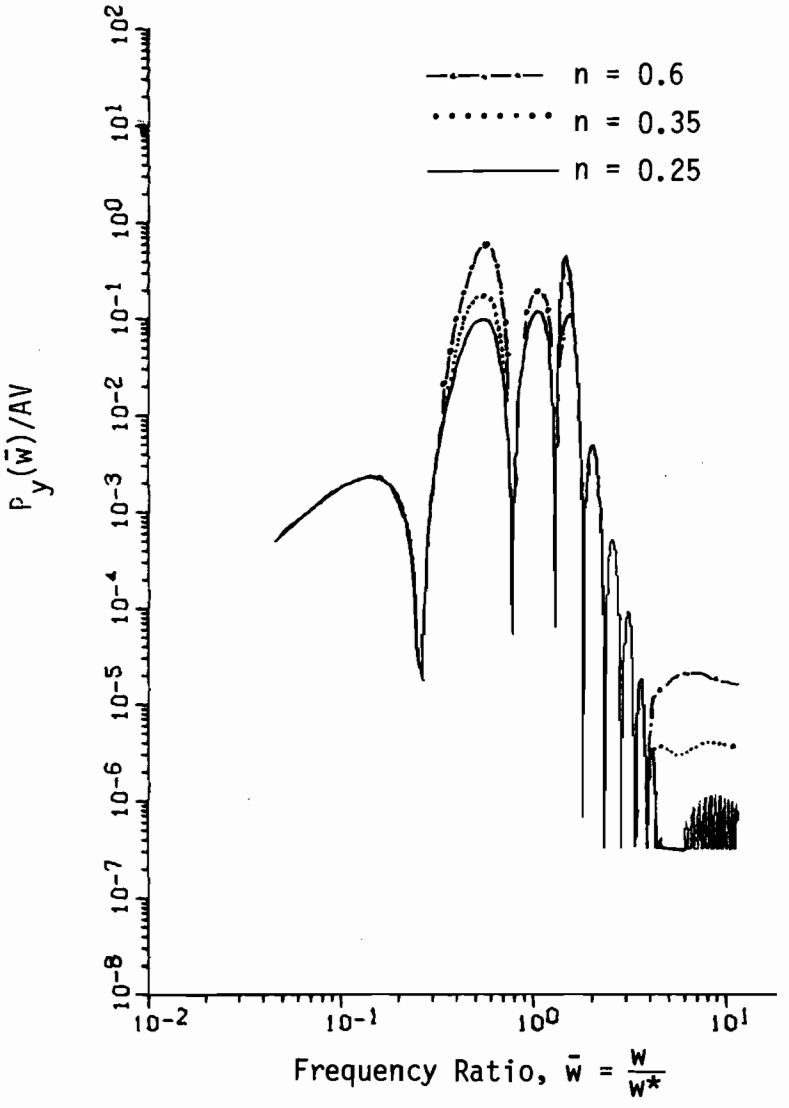

Figure 18. Normalized autospectral density of the output at vehicle center with AV/f^2 input spectra for various values of n.

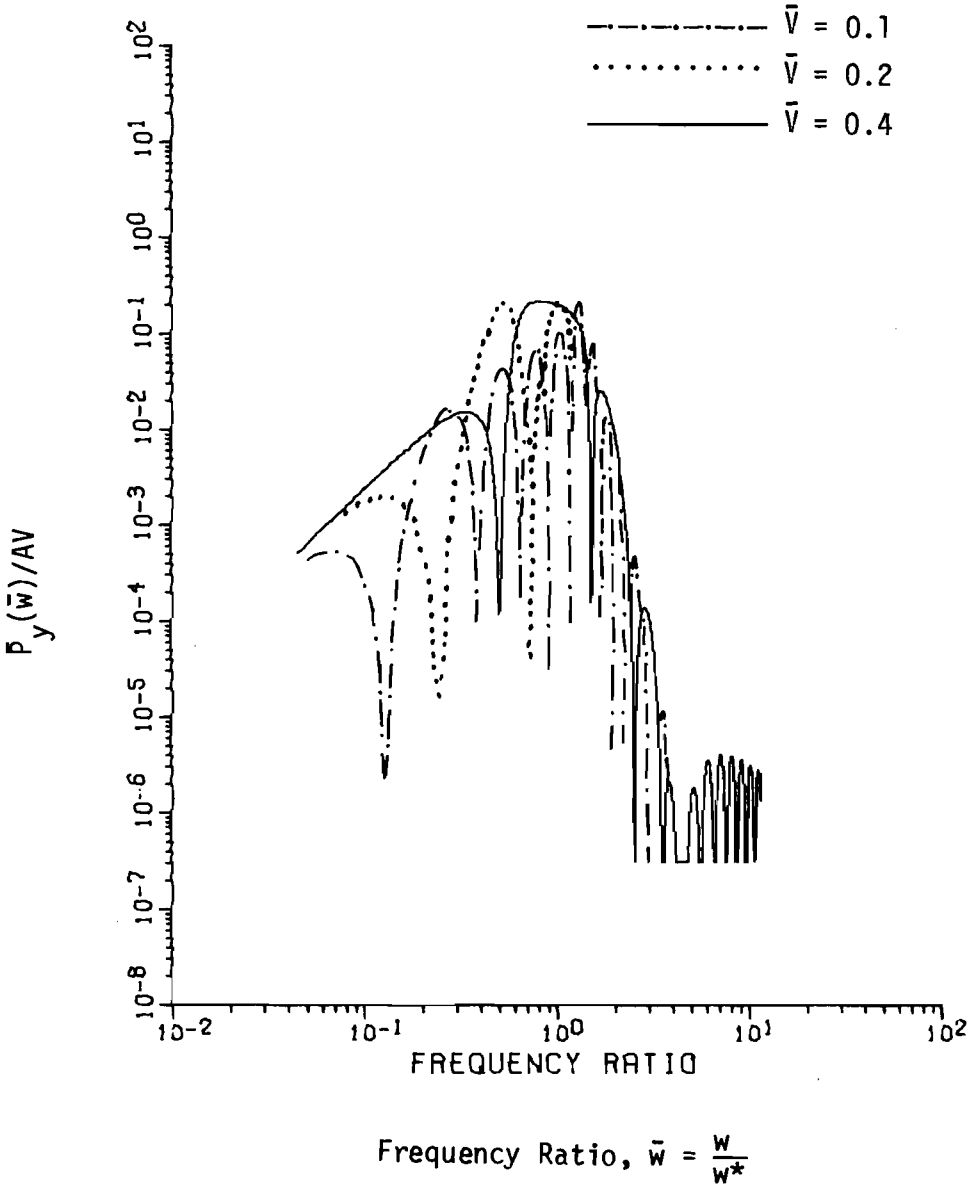

Figure 19. Normalized power spectral density of the acceleration output at vehicle center for various values of $\bar{V}$.

PART IV

CONCLUSIONS AND RECOMMENDATIONS

A lateral vehicle dynamics model has been developed which fairly accurately predicts low frequency lateral vehicle motions subject to sidewall guiding surface roughness for automated guideway transit system vehicles similar to the Dallas/Fort Worth AIRTRANS. A general nonlinear model has been developed which includes the nonlinear constitutive relationships of some of the elements built into the vehicle guidance system. The model has then been linearized for ease of ride quality simulation and study. Predicted outputs of the linearized model using two different guideway roughness models for inputs have been compared with measured vehicle accelerations and found to agree reasonably well below about 8 hertz. Motions at frequencies above this contain components due to drive train and equipment imbalance, bending and other non-rigid body modes, and other effects not included in the six-degree-of-freedom model used.

The model equations of motion have been non-dimensionalized, and a set of twelve basic independent vehicle non-dimensional parameters has been identified. Basic vehicle modes have been determined and frequencies and motions for each mode have been characterized. The lowest frequency mode occurs at about 1.6 hertz and is primarily a lateral body displacement mode. The yaw mode appears at a frequency of about 2 hertz, only a little higher.

A sensitivity study utilizing the basic non-dimensional vehicle parameters indicates that the ride quality is most sensitive to three: the steering radius ratio, the steering lever ratio, and the velocity ratio. This would indicate that the greatest effects upon the general ride quality of the vehicle can be made by changes in the vehicle steering gain and the vehicle velocity.

It is recommended that further studies be developed to include vertical motions. It is also suggested that other automated guideway transit systems be examined to determine the applicability of the model to other systems. Additionally, it is suggested that this model be coupled with studies of guideway roughness parameters and costs and with studies of ride quality

criteria and passenger sensitivity. The model may be used to relate guideway roughness and cost and vehicle parameters to ride quality criteria and passenger comfort. This will ultimately allow the determination of the relationships between passenger acceptability and guideway and vehicle costs. At that time, intelligent decisions can be made regarding ride quality and construction specifications for new systems.

APPENDICES

APPENDIX A

DERIVATION OF EQUATIONS OF MOTION

The equations of motion for the vehicle are derived on the basis of Figure 1. Consider the front guidebar and assume lateral motion only:

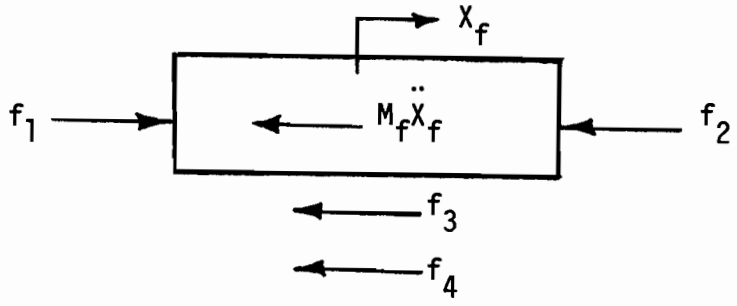

Figure A.I

Applying Newton's Second Law, gives

$$M_f\ddot{X}_f = f_1 - f_2 - f_3 - f_4 \qquad (A.1)$$

where f_1 and f_2 are spring forces from the guidewheels, f_3 is the spring force of the mechanical stop, and f_4 is the reaction force of the connecting rod. Next

$$f_1 = K_1 [U_1 - X_f] \qquad (A.2)$$

$$f_2 = K_1 [X_f - U_2] \qquad (A.3)$$

$$f_3 = K_2 [X_f - X_{b1}] \qquad (A.4)$$

where X_{b1} is the displacement of the point where the mechanical stop attaches to the vehicle. For small motions

$$X_{b1} = X_m + d_1\psi$$

where ψ is the angular rotation of the vehicle body.

Consider the rod connecting the front guidebar and the steering link as shown below:

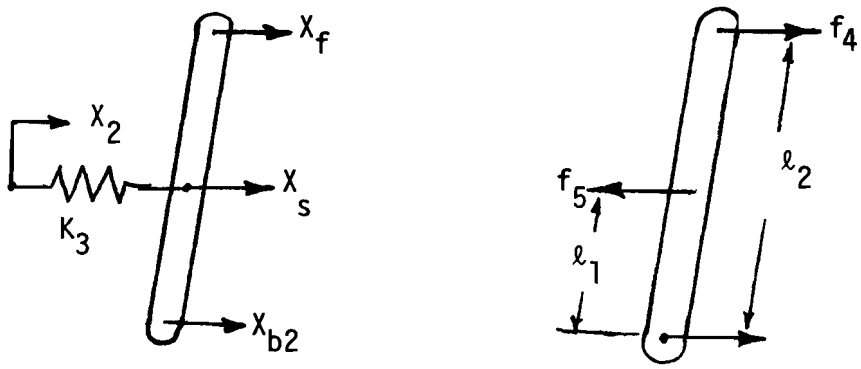

Figure A.II

$$\frac{X_f - X_{b2}}{\ell_2} = \frac{X_s - X_{b2}}{\ell_1}$$

or rearranging

$$X_s = \left(\frac{\ell_1}{\ell_2}\right)X_f - \left(\frac{\ell_1}{\ell_2}\right)X_{b2} + X_{b2} \qquad (A.5)$$

Now

$$X_2 = X_{b2} + r_1\Theta_f$$

where Θ_f is the steering angle of the front wheel, and

$$f_5 = K_3[X_s - X_2]$$

$$= K_3[(\frac{\ell_1}{\ell_2})X_f - (\frac{\ell_1}{\ell_2})X_{b2} - r_1\Theta_f] \tag{A.6}$$

Again,

$$X_{b2} = X_m + d_2\psi$$

$$\therefore \quad f_5 = K_3[(\frac{\ell_1}{\ell_2})X_f - (\frac{\ell_1}{\ell_2})X_m - (\frac{\ell_1}{\ell_2})d_2\psi - r_1\Theta_f] \tag{A.7}$$

Similarly, one can find that

$$f_4 = (\frac{\ell_1}{\ell_2})f_5$$

$$= (\frac{\ell_1}{\ell_2})K_3\,[(\frac{\ell_1}{\ell_2})X_f - (\frac{\ell_1}{\ell_2})X_m - (\frac{\ell_1}{\ell_2})d_2\psi - r_1\theta_f] \tag{A.8}$$

Therefore:

$$M_f\ddot{X}_f = K_1[U_1 - X_f] - K_1[X_f - U_2] - K_2[X_f - X_m - d_1\psi]$$

$$- \frac{\ell_1}{\ell_2}\,K_3[(\frac{\ell_1}{\ell_2})X_f - (\frac{\ell_1}{\ell_2})X_m - (\frac{\ell_1}{\ell_2})d_2\psi - r_1\Theta_f] \tag{A.9}$$

Next, consider the motion of the front steering assembly, which includes two pneumatic tires, cranks, steering links, and so on. Pneumatic tires produce a lateral force and self-aligning torque on a tire. Each of them is a function of the tire slip angle. The slip angle is defined as the angle between the velocity vector of the wheel and the wheel's diametral plane.

The lateral force and the aligning torque acting on the inside tire, respectively, are given by

$$f_x = \bar{C}[\alpha] \tag{A.10}$$

$$T_x = \bar{C}_t[\alpha] \tag{A.11}$$

where the direction of the force and torque in each case acts to decrease α. It is assumed that $\bar{C}$ and $\bar{C}_t$ are the same for all four tires. The slip angle for both front tires is considered to be the same and is found by referring to the figure below, where $\vec{V}$ is the forward velocity of the vehicle and $\vec{V}_t$ is the velocity of the tire.

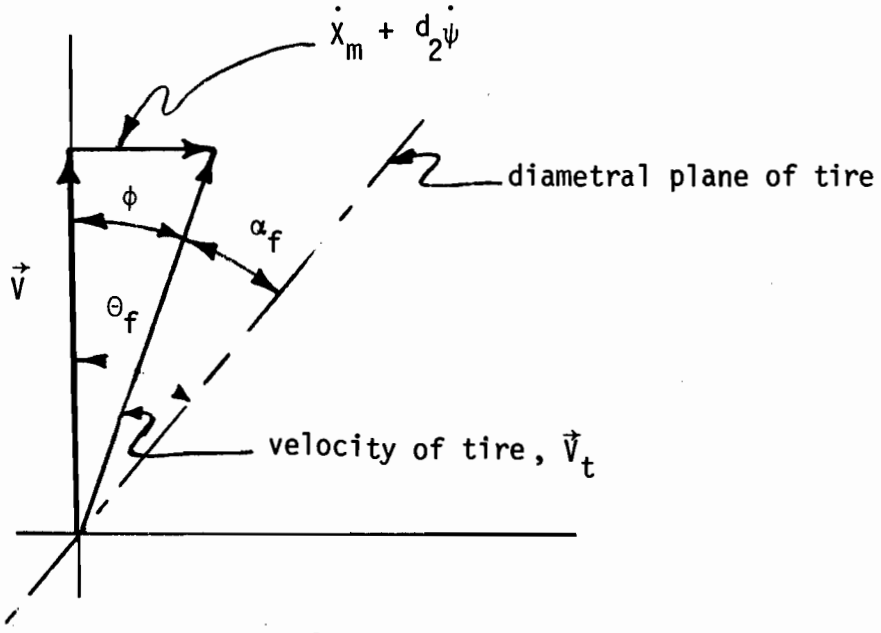

Figure A.III

From the figure

$$\tan \phi = \frac{d_2\dot{\psi} + \dot{X}_m}{V}$$

and for small angles

$$\phi \simeq \frac{d_2\dot{\psi} + \dot{X}_m}{V}$$

Therefore $$\alpha_f = \theta_f - \phi = \theta_f - \frac{\dot{X}_m + d_2\dot{\psi}}{V} \tag{A.12}$$

By a similar development, one also obtains the slip angle for the rear wheels:

$$\alpha_r = \theta_r - \frac{\dot{X}_m - d_2\dot{\psi}}{V} \tag{A.13}$$

Substituting into (A.10) and (A.11), one obtains the following for the front wheels:

$$f_f = C\alpha_f = C\left(\theta - \frac{\dot{X}_m + d_2\dot{\psi}}{V}\right) \tag{A.14}$$

$$T_f = C\left(\theta_f - \frac{\dot{X}_m + d_2\dot{\psi}}{V}\right) \tag{A.15}$$

where T_f is counterclockwise and f_f is in the positive X direction

C and C_t are double the values they would be for a single tire since the two tires on the assembly are assumed identical. Similarly, one has, for the rear wheel

$$f_r = C\left(\theta_r - \frac{\dot{X}_m - d_2\dot{\psi}}{V}\right) \tag{A.16}$$

$$T_r = C_t\left(\theta_r - \frac{X_m - d_2\dot{\psi}}{V}\right) \tag{A.17}$$

Next, consider the motion of the front steering assembly:

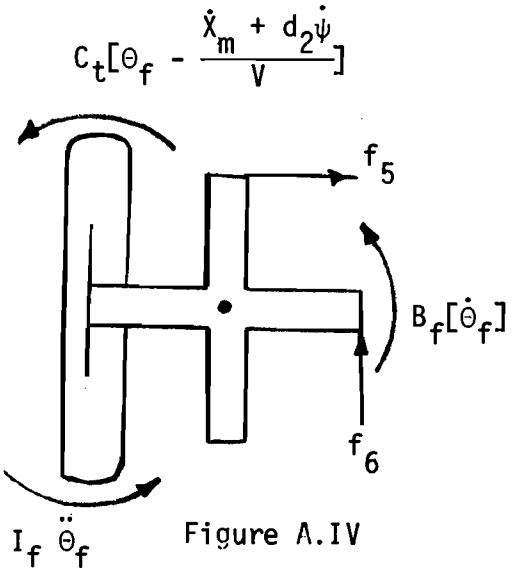

Figure A.IV

$$I_f\ddot{\theta}_f + B_f[\dot{\theta}_f] + C_t\left[\theta_f - \frac{\dot{X}_m + d_2\dot{\psi}}{V}\right] + f_6 r_2 = f_5 r_1 \qquad (A.18)$$

$$f_6 = K_4\,[r_2(\theta_f + \theta_r)] \qquad (A.19)$$

$$I_f\ddot{\theta}_f + B_f[\theta_f] + C_t\left[\theta_f - \frac{\dot{X}_m + d_2\dot{\psi}}{V}\right] + r_2K_4[r_2(\theta_f + \theta_r)]$$
$$- r_1K_3\left[\frac{\ell_1}{\ell_2}(X_f - X_m - d_2\psi) - r_1\theta_f\right] = 0 \qquad (A.20)$$

Next, consider the dynamic equilibrium of the rear steering assembly.

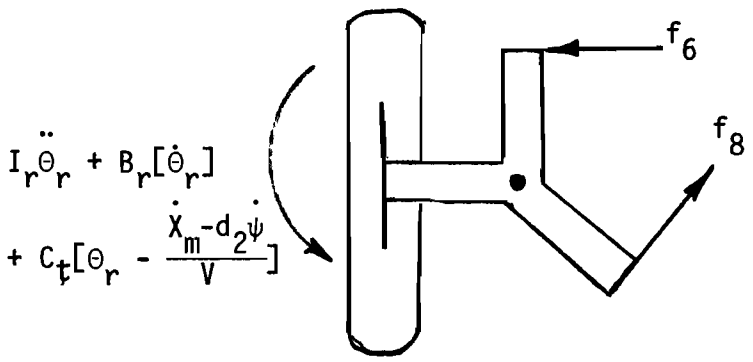

Figure A.V

$$I_r\ddot{\theta}r + B_r[\dot{\theta}_r] + C_t\left[\theta_r + \frac{\dot{X}_m - d_2\dot{\psi}}{V}\right] + f_8 r_1 + f_6 r_2 = 0 \qquad (A.21)$$

Consider the connecting rod as shown

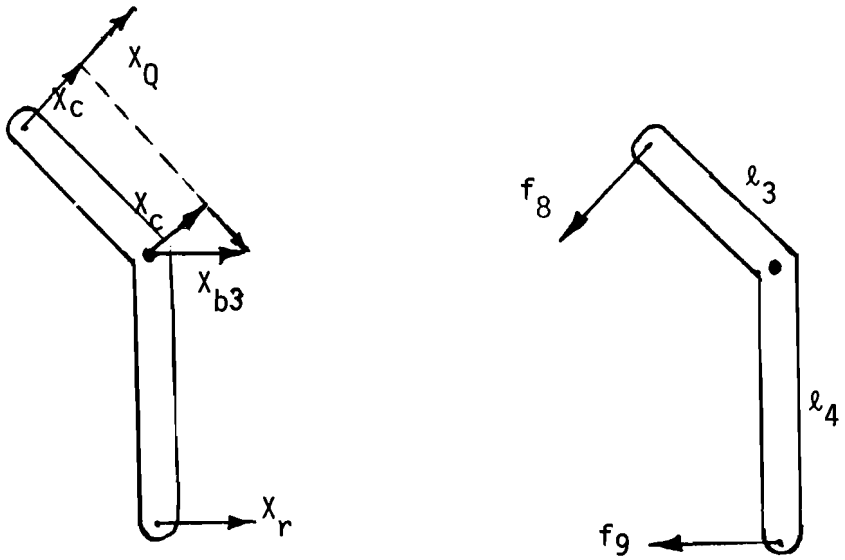

Figure A.VI

$$X_Q = \frac{\ell 3}{\ell_4}[X_{b_3} - X_r]$$

where X_Q is the motion of the end of the rod relative to the pivot point.

Now $X_{b_3} = X_m - d_2\psi$

$$X_Q = \frac{\ell_3}{\ell_4}[X_m - d_2\psi - X_r]$$

Since $f_8 = K_5[X_Q + r_1\theta_r]$

$$f_8 = K_5\left[(\frac{\ell_3}{\ell_4})X_m - (\frac{\ell_3}{\ell_4})\, d_2\psi - (\frac{\ell_3}{\ell_4})X_r + r_1\theta_r\right] \qquad (A.22)$$

and $$f_9 = (\frac{\ell_3}{\ell_4})K_5\left[(\frac{\ell_3}{\ell_4})X_m - (\frac{\ell_3}{\ell_4})d_2\psi - (\frac{\ell_3}{\ell_4})X_r + r_1\theta_r\right] \qquad (A.23)$$

Putting (A.19) and (A.22) into (A.21), one has

$$I_r\ddot{\theta}_r + B_r[\dot{\theta}_r] + C_T\left[\theta_r - \frac{\dot{X}_m - d_2\dot{\psi}}{V}\right]$$
$$+ r_1K_5\left[\left(\frac{\ell_3}{\ell_4}\right)X_m - \left(\frac{\ell_3}{\ell_4}\right)d_2\psi - \left(\frac{\ell_3}{\ell_4}\right)X_r + r_1\theta_r\right]$$
$$+ r_2K_4[r_2(\theta_f + \theta_r)] = 0 \qquad \text{(A.24)}$$

Next, consider the rear guide bar

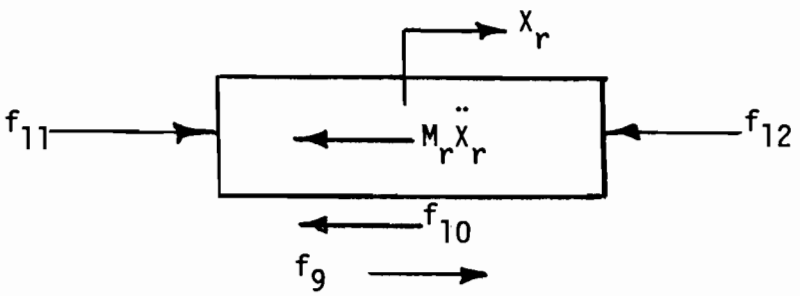

Figure A.VII

$$f_9 + f_{11} = M_r\ddot{X}_r + f_{10} + f_{12}$$

where

$$f_{11} = K_1[U_3 - X_r]$$

$$f_{12} = K_1[X_r - U_4]$$

$$f_{10} = K_2[X_r - X_{b4}]$$

$$X_{b4} = X_m - d_1\psi$$

$$M_r \ddot{X}_r = \left(\frac{\ell_3}{\ell_4}\right) K_5 \left[\left(\frac{\ell_3}{\ell_4}\right) X_m - \left(\frac{\ell_3}{\ell_4}\right) d_2 \psi - \left(\frac{\ell_3}{\ell_4}\right) X_r + r_1 \theta_r \right]$$

$$+ K_1[U_3 - X_r] - K_2[X_r - X_m + d_1\psi] - K_1[X_r - U_4] \qquad (A.25)$$

Now consider the motion of the vehicle body as diagrammed below.

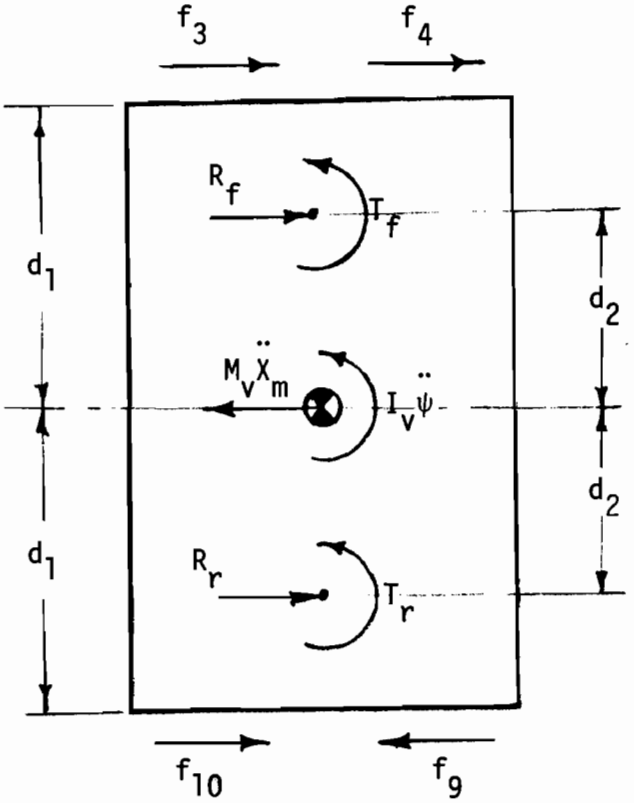

Figure A.VIII

where the forces f_3, f_4, f_9,and f_{10} are as previously defined, and where the forces R_f and R_r and torques T_f and T_r are the forces and torques applied to the vehicle by the front and rear wheel assemblies. Summing the forces shown on the diagram yields

$$m_V \ddot{X}_m = R_f + R_r + f_3 + f_4 + f_{10} - f_9 \qquad (A.26)$$

and summing the moments yields

$$I_V \ddot{\psi} - d_1(f_3 + f_4 + f_9 - f_{10}) - d_2(R_f - R_r) + T_f + T_r = 0 \quad (A.27)$$

The forces R_f and R_r are simply equal to the external forces applied to the wheels minus the mass of the wheels times their acceleration:

$$R_f = C\left[\theta_f - \frac{\dot{X}_m + d_2\dot{\psi}}{V}\right] - M_w(\ddot{X}_m + d_2\ddot{\psi}) \quad (A.28)$$

$$R_r = C\left[\theta_r - \frac{\dot{X}_m - d_2\dot{\psi}}{V}\right] - M_w(\ddot{X}_m - d_2\ddot{\psi}) \quad (A.29)$$

Similarly, the torques T_f and T_r are equal to the torques applied to the wheels externally less the torques associated with the angular acceleration of the wheels. By examination of equations (A.20) and (A.24) it can be seen that

$$T_f = -B_f[\dot{\theta}_f] - r_2K_4[r_2(\theta_f + \theta_r)] + r_1K_3\left[\left(\frac{\ell_1}{\ell_2}\right)(X_f - X_m - d_2\psi) - r_1\theta_f\right] \quad (A.30)$$

and

$$T_r = -B_r[\dot{\theta}_r] - r_2K_4[r_2(\theta_r + \theta_f)] + r_1K_3\left[\left(\frac{\ell_1}{\ell_2}\right)(X_r - X_m + d_2\psi - r_1\theta_r\right] \quad (A.31)$$

Substituting (A.28) through (A.31) into (A.26) yields

$$(M_V + 2M_w)\ddot{X}_m - C\left[\theta_f - \frac{\dot{X}_m + d_2\dot{\psi}}{V}\right]$$
$$- C\left[\theta_r - \frac{\dot{X}_m - d_2\dot{\psi}}{V}\right] - \left[\left(\frac{\ell_1}{\ell_2}\right)K_3 \quad \left(\frac{\ell_1}{\ell_2}\right)(X_f - X_m - d_2\psi) - r_1\theta_f\right]$$
$$- \left(\frac{\ell_1}{\ell_2}\right)K_3\left[\left(\frac{\ell_1}{\ell_2}\right)(X_r - X_m + d_2\psi) - r_1\theta_r\right]$$
$$- K_2[X_f - X_m - d_1\psi] - K_2[X_r - X_m + d_1\psi] = 0 \qquad \text{(A.32)}$$

and into (A.27) yields

$$(I_V + 2d_2^2M_w)\ddot{\psi} - d_2C\left[\theta_f - \frac{\dot{X}_m + d_2\dot{\psi}}{V}\right]$$
$$+ d_2C\left[\theta_r - \frac{\dot{X}_m - d_2\dot{\psi}}{V}\right] - d_1K_2[X_f - X_m - d_1\psi]$$
$$+ d_1K_2[X_r - X_m + d_1\psi] - B_w[\dot{\theta}_f] - B_w[\dot{\theta}_r]$$
$$- 2r_2K_4[r_2(\theta_r + \theta_f)]$$
$$- \left(d_1\frac{\ell_1}{\ell_2} - r_1\right)K_3\left[\left(\frac{\ell_1}{\ell_2}\right)(X_f - X_m - d_2\psi) - r_1\theta_f\right]$$
$$+ \left(d_1\frac{\ell_1}{\ell_2} + r_1\right)K_3\left[\left(\frac{\ell_1}{\ell_2}\right)(X_r - X_m + d_2\psi) - r_1\theta_r\right] = 0 \qquad \text{(A.33)}$$

Substitution of the parameters $n_f = \left(\frac{\ell_1}{\ell_2}\right)$, $n_r = \left(\frac{\ell_3}{\ell_4}\right)$, $M = (M_V + 2M_w)$, and $I = (I_V + 2d_2^2 M_w)$ results in the equations (2.1 - 2.6) defined in Chapter 2.

APPENDIX B

SIX-DEGREE-OF-FREEDOM LINEAR SYSTEM MATRICES

B.1 Dimensional System

Mass Matrix M (6x6 matrix)

$m(1,1) = m_f$ $\qquad$ $m(2,2) = m_r$

$m(3,3) = I_w$ $\qquad$ $m(4,4) = I_w$

$m(5,5) = M$ $\qquad$ $m(6,6) = I$

All terms not specified are equal to zero

Damping Matrix C (6x6 matrix)

$c(3,3) = b_w$ $\qquad$ $c(3,5) = -\frac{c_t}{V}$

$c(3,6) = -\frac{c_t d_2}{V}$ $\qquad$ $c(4,4) = b_w$

$c(4,5) = -\frac{c_t}{V}$ $\qquad$ $c(4,6) = \frac{c_t d_2}{V}$

$c(5,5) = \frac{2c}{V}$ $\qquad$ $c(6,3) = -b_w$

$c(6,4) = -b_w$ $\qquad$ $c(6,6) = \frac{2d_2^2 c}{V}$

All terms not specified are equal to zero

Stiffness Matrix K (6x6 matrix)

$k(1,1) = n_f^2 k_3 + 2k_1$ $\qquad$ $k(1,3) = -n_f r_1 k_3$

$k(1,5) = -n_f^2 k_3$ $\qquad$ $k(1,6) = -n_f^2 d_2 k_3$

$k(2,2) = n_r^2 k_3 + 2k_1$ $\qquad$ $k(2,4) = -n_r r_1 k_3$

$k(2,5) = -n_r^2 k_3$ $\qquad$ $k(2,6) = -n_r^2 d_2 k_3$

$k(3,1) = -r_1 n_f k_3$ $\qquad$ $k(3,3) = c_t + r_2^2 k_4 + r_1^2 k_3$

$k(3,4) = r_2^2 k_4$ $\qquad$ $k(3,5) = r_1 n_f k_3$

$k(3,6) = r_1 n_f d_2 k_3$ $\qquad$ $k(4,2) = -r_1 n_r k_3$

$k(4,3) = r_2^2 k_4$ $\qquad$ $k(4,4) = c_t + r_2^2 k_4 + r_1^2 k_3$

$k(4,5) = r_1 n_r k_3$ $\qquad$ $k(4,6) = -r_1 n_r d_2 k_3$

$k(5,1) = -n_f^2 k_3$ $\qquad$ $k(5,2) = -n_r^2 k_3$

$k(5,3) = -c + n_f r_1 k_3$ $\qquad$ $k(5,4) = -c + n_f r_1 k_3$

$k(5,5) = n_f^2 + n_r^2 k_3$ $\qquad$ $k(5,6) = (n_r^2 - n_f^2) d_2 k_3$

$k(6,1) = (r_1 n_f - d_1 n_f^2) k_3$ $\qquad$ $k(6,2) = -(d_1 n_r^2 + r_1 n_r) k_3$

$k(6,3) = 2r_2^2 k_4 - r_1 d_1 n_f k_3 + d_2 c$ $\qquad$ $k(6,4) = 2r_2^2 k_4 + r_1 d_1 n_r k_3 - d_2 c$

$k(6,5) = d_1 (n_r^2 - n_f^2) k_3 + r_1 (n_f + n_r) k_3$ $\qquad$ $k(6,6) = (n_f^2 + n_r^2) d_1 d_2 k_3 + (n_r - n_f) r_1 d_1 k_3$

All terms not specified above are equal to zero

Input Matrix G (6x4 matrix)

$g(1,1) = k_1$ $\qquad$ $g(1,2) = k_1$

$g(2,3) = k_1$ $\qquad$ $g(2,4) = k_1$

All terms not specified above are equal to zero

Output Matrix c^T (row vector, dimension = 12)

$$c(1) = \frac{n_f^2 k_3}{M} + \frac{(d_1 n_f - r_1) n_r \ell k_3}{I}$$

$$c(2) = \frac{n_r^2 k_3}{M} - \frac{(d_1 n_r + r_1) n_r \ell k_3}{I}$$

$$c(3) = \frac{c - n_f r_1 k_3}{M} + \frac{\ell d_2 c - \ell d_1 n_f r_1 k_3 + \ell r_1^2 k_3 + 2\ell r_2^2 k_4}{I}$$

$$c(4) = \frac{c - n_r r_1 k_3}{M} + \frac{-\ell d_2 c + \ell d_1 n_r r_1 k_3 + \ell r_1^2 k_3 + 2\ell r_2^2 k_4}{I}$$

$$c(5) = -\frac{(n_f^2 + n_r^2)k_3}{M} - \frac{d_1(n_f^2 - n_r^2)\ell k_3 - r_1(n_f + n_r)\ell k_3}{I}$$

$$c(6) = \frac{(n_r^2 - n_f^2)d_2 k_3}{M} - \frac{d_1 d_2 \ell(n_f^2 + n_f^2)k_3 + d_2 r_1 \ell(n_r - n_f)k_3}{I}$$

$$c(7) = 0$$

$$c(8) = 0$$

$$c(9) = \frac{\ell b_w}{I}$$

$$c(10) = \frac{\ell b_w}{I}$$

$$c(11) = \frac{2c}{MV}$$

$$c(12) = -\frac{2cd_2\ell}{IV}$$

B.2 Non-Dimensional System Matrices (six-degree-of-freedom model)

Non-Dimensional Mass Matrix $\bar{M}$ (6x6 matrix)

$\bar{m}(1,1) = 1$ $\quad$ $\bar{m}(2,2) = 1$

$\bar{m}(3,3) = \bar{I}_w$ $\quad$ $\bar{m}(4,4) = \bar{I}_w$

$\bar{m}(5,5) = \bar{M}$ $\quad$ $\bar{m}(6,6) = \bar{I}$

All terms not specified are equal to zero.

Non-Dimensional Damping Matrix $\bar{C}$ (6x6 matrix)

$\bar{c}(3,3) = \bar{b}_w$ $\quad$ $\bar{c}(3,5) = -\bar{C}_t\bar{r}/n\bar{V}$

$\bar{c}(3,6) = -\bar{C}_t\bar{r}/n\bar{V}$ $\quad$ $\bar{c}(4,4) = \bar{b}_w$

$\bar{c}(4,5) = -\bar{C}_t\bar{r}/n\bar{V}$ $\quad$ $\bar{c}(4,6) = \bar{C}_t\bar{r}/n\bar{V}$

$\bar{c}(5,5) = 2\bar{c}\bar{r}^2/\bar{V}$ $\quad$ $\bar{c}(6,3) = -n\bar{b}_w/\bar{r}$

$\bar{c}(6,4) = -n\bar{b}_w/\bar{r}$ $\quad$ $\bar{c}(6,6) = 2\bar{c}/\bar{V}$

All terms not specified are equal to zero.

Non-Dimensional Stiffness Matrix $\bar{K}$ (6x6 matrix)

$\bar{k}(1,1) = n^2\bar{K}_3 + 2$ $\quad$ $\bar{k}(1,3) = -n^2\bar{K}_3$

$\bar{k}(1,5) = -n^2\bar{K}_3$ $\quad$ $\bar{k}(1,6) = -n^2\bar{K}_3$

$\bar{k}(2,2) = n^2\bar{K}_3 + 2$ $\quad$ $\bar{k}(2,4) = -n^2\bar{K}_3$

$\bar{k}(2,5) = -n^2\bar{K}_3$ $\quad$ $\bar{k}(2,6) = n^2\bar{K}_3$

$\bar{k}(3,1) = -\bar{K}_3$ $\quad$ $\bar{k}(3,3) = \bar{C}_t + \bar{K}_4 + \bar{K}_3$

$\bar{k}(3,4) = \bar{K}_4$ $\quad$ $\bar{k}(3,5) = \bar{K}_3$

$\bar{k}(3,6) = \bar{K}_3$ $\quad$ $\bar{k}(4,2) = -\bar{K}_3$

$\bar{k}(4,3) = \bar{K}_4$ $\quad$ $\bar{k}(4,4) = \bar{C}_t + \bar{K}_4 + \bar{K}_3$

$\bar{k}(4,5) = \bar{K}_3$ $\quad$ $\bar{k}(4,6) = -\bar{K}_3$

All terms not specified are equal to zero.

Non-Dimensional Input Matrix $\bar{G}$ (6x4 matrix)

$\bar{g}(1,1) = 1$ $\bar{g}(1,2) = 1$

$\bar{g}(2,3) = 1$ $\bar{g}(2,4) = 1$

All terms not specified are equal to zero.

APPENDIX C

THE FOUR-DEGREE-OF-FREEDOM MODEL

C.1 Derivation of reduced set of equations

As mentioned in the text the steering link is a relatively stiff spring with a stiffness, k_3, of about 40,000 lbf/in. It thus can be modeled as a rigid massless bar connecting the guide bars and wheels. From Figure A.II and equation A.5, one has

$$X_5 = X_2 \rightarrow X_5 - X_2 = 0$$

Therefore, $$n_f X_f - n_f X_{b2} + X_{b2} - X_{b2} - r_1\theta_f = 0$$

or $$X_f - X_{b2} = \frac{r_1}{n_f}\theta_f$$

Now $$X_{b2} = X_m + d_2\psi$$

Hence, one has the first geometric constraint

$$X_f = \frac{r_1}{n_f}\theta_f + X_m + d_2\psi \qquad (C.1)$$

By similar reasoning, the second geometric constraint for the rear steering assembly is

$$X_r = \frac{r_2}{n_r}\theta_r + Xm - d_2\psi \qquad (C.2)$$

Since the steering link is considered rigid, the expression (A.7) is no longer appropriate for the force f_5 in the steering link. Substituting $f_4 = n_f f_5$, together with equations A.2-A.4 and the constant equation C.1 into A.1 and rearranging, gives

$$\frac{1}{n_f}\left[m_f\left(\frac{r_1}{n_f}\ddot{\theta}_f + \ddot{X}_m + d_2\ddot{\psi}\right) + k_2\left(\frac{r_1}{n_f}\theta_f - k_1\left(u_1 - \frac{r_1}{n_f}\theta_f - X_m - d_2\psi\right)\right.\right.$$
$$\left.\left. + k_1\left(\frac{r_1}{n_f}\theta_f + X_m + d_2\psi - u_2\right)\right)\right] = -k_3 \qquad (C.3)$$

Substituting C.3 and A.19 into A.18 and rearranging yields

$$\frac{n_f}{r_1} I_w \ddot{\theta}_f + \frac{n_f}{r_1} B_w[\dot{\theta}_f] + \frac{n_f}{r_1} c_t[\theta_f - \frac{\dot{X}_m + d_2\dot{\psi}}{V}] + n_f \frac{r_2}{r_1} k_4[r_2(\theta_f + \theta_r)]$$

$$+ m_f(\frac{r_1}{n_f} \ddot{\theta}_f + \ddot{X}_m + d_2\ddot{\psi}) + k_2[\frac{r_1}{n_f} \theta_f]$$

$$- k_1[u_1 - \frac{r_1}{n_f} \theta_f - X_m - d_2\psi] + k_1[\frac{r_1}{n_f} \theta_f + X_m + d_2\psi - u_2]$$

$$= 0 \qquad (C.4)$$

By similar development, substituting $f_q = n_r f_8$ into A.25 with the expressions on page 59 for f_{11}, f_{12}, and f_{10} and constraint equation C.2, and combining the results A.21 yields

$$\frac{n_r}{r_1} I_w \ddot{\theta}_r + \frac{n_r}{r_1} B_w[\dot{\theta}_r] + \frac{n_r}{r_1} c_t[\theta_r - \frac{\dot{X}_m - d_2\dot{\psi}}{V}] + n_r \frac{r_2}{r_1} k_4[r_2(\theta_f + \theta_r)]$$

$$+ m_r(\frac{r_2}{n_r} \ddot{\theta}_r + \ddot{X}_m - d_2\ddot{\psi}) + k_2[\frac{r_2}{n_r} \theta_r]$$

$$- k_1[u_3 - \frac{r_2}{n_r} \theta_r - X_m + d_2\psi] + k_1[\frac{r_2}{n_r} \theta_r + X_m - d_2\psi - u_4]$$

$$= 0 \qquad (C.5)$$

Substituting the constraints (C.1) and (C.2) into equation (5), the equation becomes

$$M\ddot{X}_m - c[\theta_f - \frac{\dot{X}_m + d_2\dot{\psi}}{V}] - c[\theta_r - \frac{\dot{X}_m - d_2\dot{\psi}}{V}] - \frac{n_f}{r_1} I_w \ddot{\theta}_f - \frac{n_f}{r_1} B_w[\dot{\theta}_f]$$

$$- \frac{n_f}{r_1} c_t[\theta_f - \frac{\dot{X}_m + d_2\dot{\psi}}{V}] - n_f \frac{r_2}{r_1} k_4[r_2(\theta_f + \theta_r)] - \frac{n_r}{r_1} I_w \ddot{\theta}_r$$

$$- \frac{n_r}{r_1} B_w[\dot{\theta}_r] - \frac{n_r}{r_1} c_t[\theta_r - \frac{\dot{X}_m - d_2\dot{\psi}}{V}] - n_r \frac{r_2}{r_1} k_4[r_2(\theta_f + \theta_r)]$$

$$- k_2[\frac{r_1}{n_f} \theta_f] - k_2[\frac{r_1}{n_r} \theta_r] = 0 \qquad (C.6)$$

Similarly, substitution of the constraints into equation (6) yields

$$I\ddot{\psi} - d_2 c[\theta_f - \frac{\dot{X}_m + d_2\dot{\psi}}{V}] + d_2 c[\theta_r - \frac{\dot{X}_m - d_2\dot{\psi}}{V} - d_1 k_2[\frac{r_1}{n_f} \theta_f]$$

$$+ d_1 k_2 [\frac{r_1}{n_r} \theta_r] - B_w[\dot{\theta}_f] - B_w[\dot{\theta}_r] - 2r_2 k_4 [r_2(\theta_f + \theta_r)]$$

$$- (d_1 \frac{n_f}{r_1} - 1)(I_w \ddot{\theta}_f + B_w[\dot{\theta}_f] + c_t[\theta_f - \frac{\dot{X}_m + d_2\dot{\psi}}{V}] + r_2 k_4 [r_2(\theta_f + \theta_r)])$$

$$+ (d_1 \frac{n_r}{r_1} + 1)(I_w \ddot{\theta}_r + B_w[\dot{\theta}_r] + c_t[\theta_r - \frac{\dot{X}_m - d_2\dot{\psi}}{V}] + r_2 k_4 [r_2(\theta_f + \theta_r)])$$

$$= 0 \qquad \text{(C.7)}$$

In the above equations, k_1, k_2, k_3, k_4, c, c_t and B_w are written as operators (or functions). Equations (C.4) through (C.7) form a complete set of state equations for the reduced four-degree-of-freedom model.

C.2 Linearized system matrices in dimensional form

Mass Matrix M (4x4 matrix)

$m(1,1) = \frac{n_f}{r_1} I_w + \frac{r_1}{n_f} m_f$ $\qquad$ $m(1,3) = m_f$

$m(1,4) = m_f d_2$ $\qquad$ $m(2,2) = \frac{n_r}{r_1} I_w + \frac{r_1}{n_r} m_r$

$m(2,3) = m_r$ $\qquad$ $m(2,4) = -m_r d_2$

$m(3,1) = -\frac{n_f}{r_1} I_w$ $\qquad$ $m(3,2) = -\frac{n_r}{r_1} I_w$

$m(3,3) = M$ $\qquad$ $m(4,1) = (1 - \frac{d_1 n_f}{r_1}) I_w$

$m(4,2) = (1 + \frac{d_1 n_r}{r_1}) I_w$ $\qquad$ $m(4,4) = I$

All terms not specified are equal to zero.

Damping Matrix C (4x4 matrix)

$c(1,1) = \frac{n_f}{r_1} b_w$ $\qquad$ $c(1,3) = -\frac{n_f c_t}{r_1 V}$

$c(1,4) = \frac{n_f c_t d_2}{r_1 V}$ $\qquad$ $c(2,2) = \frac{n_r}{r_1} b_w$

$$c(2,3) = -\frac{n_r c_t}{r_1 V} \qquad c(2,4) = \frac{n_r c_t d_2}{r_1 V}$$

$$c(3,1) = \frac{n_f}{r_1} b_w \qquad c(3,2) = \frac{n_r}{r_1} b_w$$

$$c(3,3) = \frac{2cr_1 + n_f c_t + n_r c_t}{r_1 V} \qquad c(4,1) = -\frac{d_1 n_f b_w}{r_1}$$

$$c(4,2) = \frac{d_1 n_r b_w}{r_1} \qquad c(4,3) = -\frac{2c_t}{V}$$

$$c(4,4) = \frac{2cd_2^2 r_1 + n_f d_1 d_2 c_t + n_r d_1 d_2 c_t}{r_1 V}$$

All terms not specified above are equal to zero.

Stiffness Matrix K (4x4 matrix)

$$k(1,1) = \frac{2r_1 k_1 + r_1 k_2}{n_f} + \frac{r_2^2 n_f k_4 + n_f c_t}{r_1} \qquad k(1,2) = \frac{r_2^2 n_f k_4}{r_1}$$

$$k(1,3) = 2k_1 \qquad k(1,4) = 2k_1 d_2$$

$$k(2,1) = \frac{r_2^2 n_r k_4}{r_1} \qquad k(2,2) = \frac{2r_2 k_1 + r_2 k_2}{n_r} + \frac{r_2^2 n_r k_4 + n_r c_t}{r_1}$$

$$k(2,3) = 2k_1 \qquad k(2,4) = -2k_1 d_2$$

$$k(3,1) = -\left(c + \frac{n_f c_t + r_2^2 n_f k_4 + r_2^2 n_r k_4}{r_1} + \frac{r_1 k_2}{n_f}\right.$$

$$k(3,2) = -\left(c + \frac{n_r c_t + (n_f + n_r) r_2^2 k_4}{r_1} + \frac{r_1 k_2}{n_r}\right)$$

$$k(4,1) = \frac{(n_r - n_f) d_1 r_2^2 k_4 + c_t (r_1 - d_1 n_f)}{r_1} - \frac{r_1 d_1 k_2}{n_f} - d_2 c$$

$$k(4,2) = \frac{(n_r - n_f) d_1 r_2^2 k_4 + (r_1 + d_1 n_r) c_t}{r_1} + \frac{r_1 d_1 k_2}{n_f} + d_2 c$$

All terms not specified are equal to zero.

Input Matrix $\underline{G}$ (4x4 matrix)

$g(1,1) = k_1$ $\qquad$ $g(1,2) = k_1$

$g(2,3) = k_1$ $\qquad$ $g(2,4) = k_1$

C.3 Linearized system matrices in non-dimensional form

Non-Dimensional Mass Matrix $\underline{\bar{M}}$ (4x4 matrix)

$\bar{m}(1,1) = n^2\bar{I}_w + 1$ $\qquad$ $\bar{m}(1,3) = 1$

$\bar{m}(1,4) = 1$ $\qquad$ $\bar{m}(2,2) = n^2\bar{I}_w + 1$

$\bar{m}(2,3) = 1$ $\qquad$ $\bar{m}(2,4) = -1$

$\bar{m}(3,1) = -n^2\bar{I}_w$ $\qquad$ $\bar{m}(3,2) = -n^2\bar{I}_w$

$\bar{m}(3,3) = \bar{M}$ $\qquad$ $\bar{m}(4,1) = n\bar{I}_w(\bar{r} - \bar{d}_1 n)$

$\bar{m}(4,2) = n\bar{I}_w(\bar{r} + \bar{d}_1 n)$ $\qquad$ $\bar{m}(4,4) = \bar{I}\bar{r}^2$

All terms not specified are equal to zero.

Non-Dimensional Damping Matrix $\underline{\bar{C}}$ (4x4 matrix)

$\bar{c}(1,1) = -n^2\bar{b}_w$ $\qquad$ $\bar{c}(1,3) = n\bar{C}_t\bar{r}/\bar{V}$

$\bar{c}(1,4) = n\bar{C}_t\bar{r}/\bar{V}$ $\qquad$ $\bar{c}(2,2) = -n^2\bar{b}_w$

$\bar{c}(2,3) = n\bar{C}_t\bar{r}/\bar{V}$ $\qquad$ $\bar{c}(2,4) = -n\bar{C}_t\bar{r}/\bar{V}$

$\bar{c}(3,1) = n^2\bar{b}_w$ $\qquad$ $\bar{c}(3,2) = n^2\bar{d}_1\bar{b}_w$

$\bar{c}(3,3) = \dfrac{-2(\bar{c}\bar{r}^2 + n\bar{C}_t\bar{r})}{\bar{V}}$ $\qquad$ $\bar{c}(4,1) = n^2\bar{d}_1\bar{b}_w$

$\bar{c}(4,2) = -n^2\bar{d}_1\bar{b}_w$ $\qquad$ $\bar{c}(4,3) = 2\bar{C}_t\bar{r}^2/\bar{V}$

$\bar{c}(4,4) = -2(\bar{c}\bar{r}^2 + \bar{C}_t\bar{d}_1 n\bar{r})/\bar{V}$

All terms not specified are equal to zero.

Non-Dimensional Stiffness Matrix $\bar{K}$ (4x4 matrix)

$\bar{k}(1,1) = -(n^2\bar{K}_4 + n^2\bar{C}_t + 2)$ $\quad$ $\bar{k}(1,2) = -n^2\bar{K}_4$

$\bar{k}(1,3) = -2$ $\quad$ $\bar{k}(1,4) = -2$

$\bar{k}(2,1) = -n^2\bar{K}_4$ $\quad$ $\bar{k}(2,2) = -(n^2\bar{K}_4 + n^2\bar{C}_t + 2)$

$\bar{k}(2,3) = -2$ $\quad$ $\bar{k}(2,4) = 2$

$\bar{k}(3,1) = n\bar{r}\bar{c} + n^2\bar{C}_t + 2n^2\bar{K}_4$ $\quad$ $\bar{k}(3,2) = n\bar{r}\bar{c} + n^2\bar{C}_t + 2\cdot n^2\bar{K}_4$

$\bar{k}(4,1) = n\bar{r}\bar{c} + \bar{C}_t n(\bar{d}_1 n - \bar{r})$ $\quad$ $\bar{k}(4,2) = -(n\bar{r}\bar{c} + n\bar{C}_t(\bar{d}_1 n + \bar{r}))$

All terms not specified are equal to zero.

Non-Dimensional Input Matrix $\bar{G}$ (4x4 matrix)

$\bar{g}(1,1) = 1$ $\quad$ $\bar{g}(1,2) = 1$

$\bar{g}(2,3) = 1$ $\quad$ $\bar{g}(2,4) = 1$

All terms not specified are equal to zero.

BIBLIOGRAPHY

Clark, S. K., Editor, "Mechanics of Pneumatic Tires," NBS Monograph 122, November 1971.

Healey, A. J., "Ride Quality Assessment for the AIRTRANS System," Report No. MEUT-1, under contract no. DOT-OS-50126, Mechanical Engineering Department, The University of Texas at Austin, 1976.

Kao, Mike Pen-Mu, "Vehicle Ride Quality Simulation - FFT vs. Time Domain," Master's Thesis, Department of Mechanical Engineering, The University of Texas at Austin, 1975.

Murray, W. R. and C. C. Smith, "Guideway Sidewall Roughness and Guidewheel Spring Compressions of the Dallas/Fort Worth AIRTRANS," Research Report RR-42, Council for Advanced Transportation Studies, The University of Texas at Austin, 1976.

Richardson, H. H., et al, "Dynamics of Simple Air-Supported Vehicles Operating over Irregular Guideways," Report DSR 76110-4 Massachusetts Institute of Technology, Clearinghouse No. PB 173655, June 1967, p. 9.

ABOUT THE AUTHORS

CRAIG C. SMITH was born in Provo, Utah, on May 1, 1944, the son of George Clinton and Metta Crawford Smith. He obtained his primary and secondary education in Blackfoot, Idaho, where he lived during most of his childhood years. He holds B.S.M.E. and M.S. degrees from Brigham Young University and a Ph.D. degree from the Massachusetts Institute of Technology. He has worked during summers for United States Steel Corporation and Bell Telephone Laboratories as well as having other shorter term industrial consulting experience. He has been involved in transportation related studies primarily related to vehicle and guideway dynamics beginning during his graduate work at M.I.T. He has been an Instructor at Brigham Young University, and is presently Assistant Professor of Mechanical Engineering at The University of Texas at Austin where he has been since September, 1973. He has taught courses covering a variety of topics, specializing in the areas of systems dynamics, control systems, machine design, and vibrations.

STEVEN TSAO was born in Shanghai, China, on January 8, 1949. He left China and came to Hong Kong in 1960. After finishing his high school education in Hong Kong, he came to America in August, 1971, to study at Northeast Louisiana University majoring in Pharmacy. In January, 1973, he transferred to the Polytechnic Institute of Brooklyn in New York, majoring in mechanical engineering. He transferred again to the University of Texas at Austin where he received his Bachelor of Science degree with highest honors in Mechanical Engineering in May, 1975. Currently, he is a graduate student at the University of Texas at Austin and expects to receive his Master of Science degree in Mechanical Engineering in May, 1977.

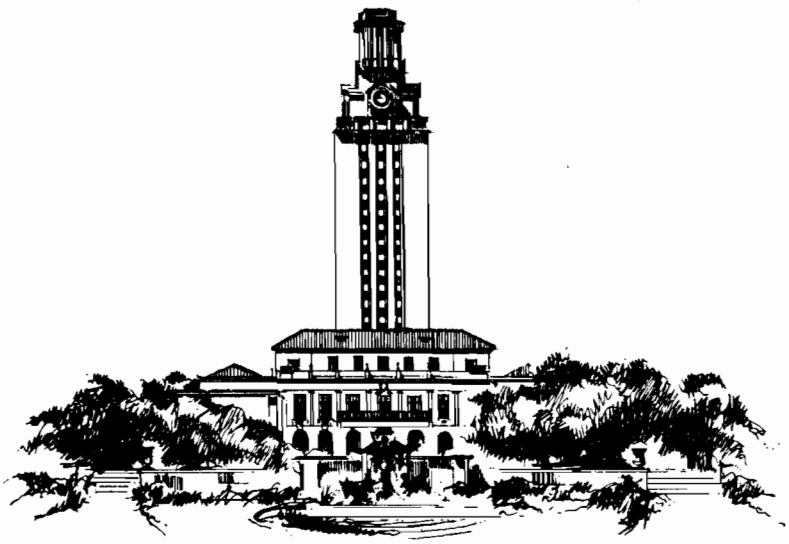

Council for Advanced Transportation Studies

THE UNIVERSITY OF TEXAS AT AUSTIN